This paper is available on line at http://www.mcponline.org

Label-free Quantitative Proteomics Reveals a Role for the *Mycobacterium tuberculosis* SecA2 Pathway in Exporting Solute Binding Proteins and Mce Transporters to the Cell Wall*[S]

Meghan E. Feltcher‡¶¶, Harsha P. Gunawardena§¶¶, Katelyn E. Zulauf‡¶¶, Seidu Malik‡, Jennifer E. Griffin¶, Christopher M. Sassetti¶‖, Xian Chen§, and Miriam Braunstein‡****

Mycobacterium tuberculosis **is an example of a bacterial pathogen with a specialized SecA2-dependent protein export system that contributes to its virulence. Our understanding of the mechanistic basis of SecA2-dependent export and the role(s) of the SecA2 pathway in *M. tuberculosis* pathogenesis has been hindered by our limited knowledge of the proteins exported by the pathway. Here, we set out to identify *M. tuberculosis* proteins that use the SecA2 pathway for their export from the bacterial cytoplasm to the cell wall. Using label-free quantitative proteomics involving spectral counting, we compared the cell wall and cytoplasmic proteomes of wild type *M. tuberculosis* to that of a Δ*secA2* mutant. This work revealed a role for the *M. tuberculosis* SecA2 pathway in the cell wall localization of solute binding proteins that work with ABC transporters to import solutes. Another discovery was a profound effect of SecA2 on the cell wall localization of the Mce1 and Mce4 lipid transporters, which contribute to *M. tuberculosis* virulence. In addition to the effects on solute binding proteins and Mce transporter export, our label-free quantitative analysis revealed an unexpected relationship between SecA2 and the hypoxia-induced DosR regulon, which is associated with *M. tuberculosis* latency. Nearly half of the transcriptionally controlled DosR regulon of cytoplasmic proteins were detected at higher levels in the Δ*secA2* mutant *versus* wild type *M. tuberculosis*. By increasing the list of *M. tuberculosis* proteins known to be affected by the SecA2 pathway, this study expands our appreciation of the types of proteins exported by this pathway and guides our understanding of the mechanism of SecA2-dependent protein export in mycobacteria. At the same time, the newly identified SecA2-dependent proteins are helpful for understanding the significance of this pathway to *M. tuberculosis* virulence and physiology.** ***Molecular & Cellular Proteomics 14: 10.1074/mcp.M114.044685, 1501–1516, 2015.***

Mycobacterium tuberculosis, the etiological agent of tuberculosis, remains a severe health concern, infecting an estimated one-third of the global population and causing an approximated 1.3 million deaths annually (1). Following inhalation into the lung, *M. tuberculosis* bacilli are engulfed by macrophages, which fail to destroy the pathogen and instead provide a niche for *M. tuberculosis* replication (2). *M. tuberculosis* proteins that are exported from the cytoplasm to the bacterial cell wall or into the host environment are ideally positioned for host-pathogen interactions or physiologic processes important to infection, such as nutrient uptake and cell wall biogenesis (3). *M. tuberculosis* has several systems for exporting proteins to extracytoplasmic locations, one of which is the SecA2-dependent protein export pathway (4). In *M. tuberculosis*, SecA2 is required for virulence in both mice and macrophage models of infection, making the identification of SecA2-dependent exported proteins important for understanding *M. tuberculosis* pathogenesis (5–7).

Mycobacteria, including *M. tuberculosis,* are among a select group of bacteria that have two nonredundant SecA ATPases, known as SecA1 and SecA2 (8). SecA1 is the housekeeping SecA, conserved throughout bacteria, and a central component of the essential general secretion (Sec) pathway. SecA1 powers translocation of unfolded proteins

From the ‡Department of Microbiology and Immunology, §Department of Biochemistry and Biophysics, University of North Carolina at Chapel Hill, North Carolina, 27599; ¶Department of Microbiology and Physiological Systems, University of Massachusetts Medical School, Worcester, Massachusetts 01655; ‖Howard Hughes Medical Institute, Chevy Chase, Maryland, 20815

Received, September 17, 2014 and in revised form, March 25, 2015
Published, MCP Papers in Press, March 26, 2015, DOI 10.1074/mcp.M114.044685

Author contributions: M.E.F., H.P.G., K.E.Z., X.C., and M.B. designed research; M.E.F., H.P.G., K.E.Z., and S.M. performed research; J.E.G. and C.M.S. contributed new reagents or analytic tools; M.E.F., H.P.G., K.E.Z., and M.B. analyzed data; M.E.F., K.E.Z., S.M., H.P.G., X.C., and M.B. wrote the paper.

across a cytoplasmic membrane channel comprised of SecYEG proteins. Proteins exported by SecA1/SecYEG possess N-terminal Sec signal peptides that are cleaved following export to liberate the mature protein. In bacteria with two SecA proteins, SecA2 is generally nonessential but required for export of a limited set of proteins and, in the case of bacterial pathogens, SecA2 often contributes to virulence (8, 9). Bacterial SecA2 systems fall into two main groups based on the membrane channel they work with and the types of substrates they transport. One type of system, called a SecA2-SecY2 system, uses an accessory SecY2 channel protein and appears to be dedicated to exporting a single glycosylated protein (10–13). The other type of system, which is the case in mycobacteria, does not include an accessory SecY and the repertoire of exported proteins is more diverse (5, 14–17). In these SecA2-only or multisubstrate SecA2 systems, SecA2 appears to work with the SecYEG channel for protein translocation (9, 17–20). Studies conducted in mycobacteria suggest that the proteins exported by its SecA2-only pathway have a tendency to fold in the cytoplasm prior to export, which distinguishes them from proteins that remain unfolded and are exclusively exported by SecA1. This folding feature of SecA2-exported proteins may dictate the need for SecA2 in their export (21).

In mycobacteria, and more specifically *M. tuberculosis*, the number of known SecA2-dependent proteins remains small. In the nonpathogenic *Mycobacterium smegmatis*, there are two cell wall proteins that are well-established as being exported via the SecA2 pathway: Ms1704 and Ms1712 (15, 20, 21). Both of these proteins are lipoproteins with Sec signal peptides and members of the solute-binding protein (SBP) family (15). SBPs are cell wall proteins that work with membrane localized ABC transporters to import solutes into the bacterial cytoplasm. Like all mycobacteria, *Mycobacterium marinum*, a pathogen of fish and frogs, also has a SecA2-only system (16, 22). As many as 40 *M. marinum* proteins are predicted by proteomics to be SecA2-dependent (16). The most striking finding of this *M. marinum* study is that PknG, a protein associated with virulence and lacking a Sec signal peptide, is reduced in abundance in a cell envelope fraction of a *M. marinum secA2* mutant compared with wild type (16, 23, 24). There are no direct orthologs of Ms1704 and Ms1712 in *M. tuberculosis* and the mode of PknG export by *M. tuberculosis* has not been established. Past efforts to identify SecA2-dependent proteins in *M. tuberculosis* are limited to comparative two-dimensional gel electrophoresis (2D-GE) of fully secreted proteins. With this approach, superoxide dismutase SodA (5) was identified as a protein requiring SecA2 for its secretion. Like PknG, SodA lacks a predicted Sec signal peptide. However, because inadequate SodA secretion is insufficient to explain the virulence defect of a *M. tuberculosis* Δ*secA2* mutant (7), there must exist additional *M. tuberculosis* SecA2-dependent proteins. Here, we set out to identify *M. tuberculosis* proteins dependent on SecA2 for their export by comparing the cell wall and cytoplasmic proteomes of *M. tuberculosis* wild type and a Δ*secA2* mutant using label-free quantitative (LFQ)[1] shotgun proteomics.

Our LFQ analysis revealed reduced cell wall levels of almost all of the predicted *M. tuberculosis* SBPs in the Δ*secA2* mutant *versus* wild type, suggesting a broad role for SecA2 in the export of this family of proteins. Further, multiple protein components of Mce1 and Mce4 transporters were reduced in the Δ*secA2* mutant cell wall, suggesting a dependence on SecA2 for cell wall localization of these transport systems. Our proteomics approach also revealed an unexpected role for SecA2 in the DosR-regulated stress response of *M. tuberculosis*, with higher abundance of many cytoplasmic DosR-dependent proteins detected in the Δ*secA2* mutant compared with wild type. Finally, we obtained data consistent with *M. tuberculosis* PknG being exported by the SecA2 pathway. By expanding our knowledge of the types of proteins exported by the mycobacterial SecA2 system, this study helps our effort to understand the mechanism of this specialized protein export pathway. At the same time, the SecA2-dependent proteins identified in this work provide valuable insight into potential role(s) of the SecA2 pathway in *M. tuberculosis* virulence and physiology.

EXPERIMENTAL PROCEDURES

M. tuberculosis Strains and Plasmids Used in this Study—The following *M. tuberculosis* strains were used in this study: H37Rv (wild type), mc^{2}3112 (Δ*secA2*), and a complemented strain MBTB476 (mc^{2}3112, pSM15) (5). Plasmid pSM15 is a derivative of pMV306.kan that carries the *M. tuberculosis secA2* gene under the control of the *hsp60* promoter. In experiments involving the complemented strain, H37Rv and Δ*secA2* strains carried the empty pMV261.kan plasmid to allow all strains to be grown in the presence of kanamycin.

Growth Conditions—*M. tuberculosis* strains were first grown at 37 °C in Middlebrook 7H9 medium (Difco, Sparks, MO) supplemented with 0.5% glycerol, 1× ADS [0.5% bovine serum albumin, 0.2% glucose, 0.85% NaCl], 0.05% Tyloxapol (Sigma St. Louis, MO), and 20 μg/ml kanamycin, if necessary. After reaching an OD_{600} of 2, cells were centrifuged and twice washed in modified 7H9 media: Middlebrook 7H9 supplemented with 0.1% glycerol, 1 mM propionic acid (Sigma), 0.5% bovine serum albumin, 0.1% Tyloxapol, pH adjusted to 6.5 and buffered with 100 mM 2-(4-morpholino)-ethane sulfonic acid. This modified 7H9 media was used in all subsequent steps of preparing samples and was designed to reflect features of the host environment encountered by *M. tuberculosis*. During infection, *M. tuberculosis* is exposed to a mildly acidic pH of 6.5 in a macrophage (25) and utilizes fatty acids as a carbon source (26–28). Washed cells were used to inoculate modified 7H9 medium at an OD_{600} of 0.08. Upon reaching an OD_{600} of 1.0, the cells were pelleted, washed with 1× phosphate-buffered saline (PBS) and sterilized by gamma-irradiation in a JL Shephard Mark I 137Cs irradiator (Department of Radiobiology, University of North Carolina at Chapel Hill) prior to removal

[1] The abbreviations used are: the following: LFQ, label-free quantitation; 2D-GE, 2-dimensional gel electrophoresis; ADS, albumin-dextrose-saline; WCL, whole cell lysate; CW, cell wall; SOL, soluble; FDR, false discovery rate; ETD, electron transfer dissociation; HCD, higher energy collision dissociation; MIPS, monoisotopic precursor ion selection.

from BSL-3 containment. In some experiments, a 40 ml volume of cells in modified 7H9 medium (OD_{600} of 0.8–1.0) was transferred to a 50 ml conical tube and let stand at 37 °C for 2 or 24 h as a strategy to induce the DosR-dependent regulon (29).

Preparation of Subcellular Fractions—Subcellular fractions were isolated as previously described (30). Briefly, irradiated cells suspended in 1× PBS containing protease inhibitors were lysed by passage through a French pressure cell. Unlysed cells were removed by centrifugation at 3000 × *g* to generate clarified whole cell lysates (WCLs), which were then spun at 27,000 × *g* for 30 min to pellet the cell wall fraction. The supernatant was then spun at 100,000 × *g* for 2 h to separate the cytoplasmic membrane fraction and collect the soluble cytoplasm-containing fraction. Protein concentrations were determined by bicinchoninic acid assay (Pierce, Rockford, IL).

SDS-PAGE Separation and In-gel Trypsin Digestion of Proteins—Cell wall proteins (34 μg) and cytoplasmic proteins (91 μg) from three biological replicates each of H37Rv and the Δ*secA2* mutant were separated on individual lanes of a precast 12% SDS-PAGE gel. Protein bands were visualized by Coomassie Blue R-250 staining (Bio-Rad, Hercules, CA) and each lane was cut into 32 gel slices for cell wall samples and 10 gel slices for cytoplasmic samples. In-gel trypsin digestion was performed, as previously described (31), with each gel slice being processed individually in a single well of a 96-well polypropylene plate. Peptides were stored at −80 °C until lyophilized.

Liquid Chromatography and Tandem Mass Spectrometry Analysis—Peptides were desalted using PepClean C18 spin columns (Pierce, Rockford, IL) and resuspended in an aqueous solution of 0.1% formic acid. Samples were analyzed by reversed phase LC-MS/MS using a 2D-nanoLC ultra system (Eksigent Inc, Dublin, CA) coupled to an LTQ-Orbitrap XL system with ETD (Thermo Scientific, San Jose, CA). The Eksigent system was configured to trap and elute peptides in 1D mode of operation via a sandwiched injection of ~250 fmol of sample. The trapping was performed on a 3 cm long 100 μm i.d. C18 column, whereas elution was performed on a 15 cm long 75 μm i.d., 5 μm, 300Å particle; ProteoPep II integraFrit C18 column (New Objective Inc, Woburn, MA). Analytical separation of tryptic peptides was achieved with a linear gradient of 2–40% over 120 min at a 200 nL/min flow rate, where buffer A is aqueous solution of 0.1% formic acid and buffer B is a solution of acetonitrile in 0.1% formic acid. Mass spectrometric data acquisition was performed in a data dependent manner. A full scan mass analysis on an LTQ-Orbitrap (externally calibrated to a mass accuracy of < 1 ppm, and resolution of 60,000 at 400 Th) was followed by intensity dependent MS/MS of the 10 most abundant peptide ions. The dynamic exclusion time window was set to 60 s with monoisotopic precursor ion selection (MIPS) and charge state screening enabled for charges $\geq +2$ for triggering data dependent MS/MS scans.

Peptide and Protein Identification—Mass spectra were processed, and peptide identification was performed using Mascot ver. 2.3 (Matrix Science Inc., Boston, MA) implemented on Proteome Discoverer ver. 1.3 (Thermo-Fisher Scientific, San Jose, CA). All searches were performed against the National Center for Biotechnology (NCBI) *M. tuberculosis* H37Rv protein sequence database (RefSeq NC_000962 uid 57777, 3906 protein entries). Peptides were identified using a target-decoy approach with a peptide false discovery rate (FDR) of 1% (32, 33). A precursor ion mass tolerance of 200 p.p.m. and a product ion mass tolerance of 0.5 Da (34) were used during the search to increase search space and reduce false-positive identifications with a maximum of two missed trypsin cleavage sites and oxidation of methionine residues as dynamic modification.

Peptide Validation and Spectral Count-based Label-free Quantitation (LFQ)—Peptide and protein validation and label-free spectral count-based quantitation was performed using ProteoIQ: ver 2.3.02 (PREMIER Biosoft international, Palo Alto, CA). Mascot search engine results against forward and decoy *M. tuberculosis* databases were obtained for all RAW data. Both forward and decoy search results were imported as DAT files into ProteoIQ to asses FDR. A peptide FDR of 1% and protein FDR of 5% were used to filter valid spectra. Peptide assignment to proteins was achieved by considering Occam's Razor principle that takes into account the presence of protein groups and penalizes proteins containing peptides identified in multiple proteins. The PROVALT algorithm in ProteoIQ was used to determine ion score thresholds and protein FDR (33). Mascot protein identifications were also subjected to probability-based confidence measurements using an independent implementation of the statistical models commonly known as peptide and protein Prophet deployed in ProteoIQ (35, 36). All protein hits were filtered with peptide Prophet using a minimum probability threshold of 0.5. Evaluation of sensitivity and error rates in this filtered data set for the cell wall proteome showed a sensitivity of 95% with a 4.8% error rate whereas the filtered data for the cytoplasm had 90% sensitivity with a 6.2% error rate. From a total of 2194 proteins detected in the cell wall and 2226 detected in cytoplasmic samples the data was filtered for proteins identified by a minimum of two peptides resulting in 1729 cell wall and 1810 cytoplasmic proteins identified, reported, and used in all further analysis in this study.

Relative protein quantitation was performed using spectral count-based LFQ. For each biological sample, data from the individual gel slices were combined. Statistical analysis was performed on all proteins identified with average spectral counts of ≥4 among the three replicates of at least one strain. The spectral count data was normalized by total spectral counts in each sample, using ProteoIQ, to adjust for differences in overall protein levels between samples. The normalized spectral count data was then used to calculate a ratio of the average spectral counts obtained for each strain ΔsecA2/H37Rv. Proteins were considered to have a significant difference in abundance if there was a difference of twofold or greater in average spectral counts between strains and a p value ≤ 0.01 using an unpaired two-tailed Student's t test. Multiple hypothesis testing was also applied to the data by computing q values using QVALUE software (http://genomics.princeton.edu/storeylab/qvalue/). The q values for quantitated proteins are reported on the data tables. The q value is an estimate of the minimum FDR for proteins judged to be significantly changed at a given p value (in our case $p \leq 0.01$) (37). Spectral counts for all proteins and peptides identified in each replicate sample is provided in supplemental Tables S2 and S8 for cell wall identifications and supplemental Tables S9 and S15 for cytoplasmic identifications. For the proteins selected for relative quantitation (≥4 average spectral counts) spectral count data and statistics across replicates are shown in supplemental Tables S3–S7 for cell wall fractions and supplemental Tables S10–S14 for cytoplasmic fractions.

Immunoblotting—Equal protein content for whole cell lysates, cell wall, or cytoplasmic fractions from H37Rv, Δ*secA2* mutant, and the complemented strain were separated by SDS-PAGE and then transferred to nitrocellulose membranes. After blocking for 1 h at room temperature, proteins were detected using the following antibodies: antiMce1A at 1:10,000, antiMce1C at 1:5000, antiMce1F at 1:10,000, antiLprK at 1:5000, anti19kD at 1:20,000 (provided by Douglas Young, Imperial College, United Kingdom), antiPhoS1 at 1:20,000 (IT23, NIH Biodefense and Emerging Infections Research Resources Repository, NIAID), antiPknG at 1:5000 (provided by Yossef Av-Gay, University of British Columbia, Canada), and antiHspX at 1:1000 (IT20, NIH Biodefense and Emerging Infections Research Resources Repository, NIAID). Anti-mouse and anti-rabbit IgG conjugated horseradish peroxidase (Bio-Rad, Hercules, CA) secondary antibodies were used and signal was detected using Western Lightning Chemiluminescent detection reagent (Perkin-Elmer, Waltham, MA).

AntiMce Antibody Production—Antipeptide antibodies for Mce1A, 1C, 1F, and LprK were generated in rabbits using peptides conjugated to keyhole limpet hemocyanin by Open Biosystems (Huntsville, AL). The peptides used were the following: GRVDTISEVTRDGESA (Mce1A), DLLVDRKEDLAETLTILGR (Mce1C), SAVYSPASGELVGPDGVKY (Mce1F), and DPSPVPLKDGDTIPLKRS (LprK). Immunoaffinity chromatography was used for antibody purification.

Bioinformatic Analysis—Sec signal peptides were predicted using Signal P 4.01 and default options for Gram-positive bacteria (38). Tat signal peptide predictions were compiled using TatP 1.03, TATFIND v1.44, and TigrFAM5 (39–42). Transmembrane predictions were made using TMHMM 2.06 (43). Mycobacterial lipoproteins were predicted using the list compiled by Sutcliffe and Harrington (44). Protein associations were predicted using the Search Tool for the Retrieval of Interacting Genes/Proteins (STRING) (version 9.1) set for a medium confidence level (0.4) (45).

Quantitative Real-Time PCR—Triplicate cultures were grown in modified 7H9 medium to an OD_{600} of 1.0 and pelleted by centrifugation at 3000 rpm for 10 min. Bacteria were lysed in 1 ml 3:1 chloroform-methanol, then vortexed with 5 ml TRIzol (Invitrogen) and incubated for 10 min at room temperature. Phases were separated by centrifugation at 3000 rpm for 15 min at 4 °C, and RNA was precipitated from the upper phase using 1× volume of isopropanol. RNA was pelleted by centrifugation at 12,000 rpm for 30 min at 4 °C, washed twice with cold 70% ethanol, and resuspended in RNase-free water. RNA samples were treated with DNase (Promega, Madison, WI) and then column purified (Zymo RNA clean and concentrator kit). Following RNA isolation, cDNA was synthesized with random primers using the iScript cDNA Synthesis Kit (Bio-Rad). Real-time PCR was completed using 25 ng of cDNA template in triplicate technical replicates using the SensiMix SYBR and fluorescein kit (Bioline, Tauton, MA). Transcripts were normalized to the housekeeping gene *sigA* (46). Primer sequences are provided (supplemental Table S1).

RESULTS

Proteomic Analysis of Differentially Abundant Proteins in the Cell Wall of H37Rv (wild type) versus ΔsecA2 Mutant M. tuberculosis—Triplicate cultures of *M. tuberculosis* H37Rv (wild type) and Δ*secA2* mutant were grown to mid-log phase, at which time cells were sterilized by gamma irradiation and lysed with a French pressure cell to generate whole cell lysates (WCL). WCLs were then subjected to differential ultracentrifugation to generate cell wall fractions. Immmunoblot analysis of the cell wall fractions showed the presence of the 19 kDa lipoprotein but not the cytoplasmic SigA and MtrA proteins, as expected (data not shown).

Because cell wall proteins often exhibit solubility problems, we combined SDS-solubilization and SDS-PAGE separation of cell wall fractions with LC-MS/MS to analyze the cell wall proteomes, as previously described (30). For each biological replicate, cell wall proteins were collected from an entire lane of an SDS-PAGE gel in 32 slices of equal size. Tryptic peptides from each slice were analyzed separately by LC-MS/MS. In total, we identified 1729 proteins with a minimum of two unique peptides among the cell wall fractions of H37Rv (wild type) and the Δ*secA2* mutant (supplemental Table S2). These cell wall-associated proteins fall into diverse functional categories (Fig. 1). The largest functional groups of proteins identified are predicted to be involved in cell wall processes,

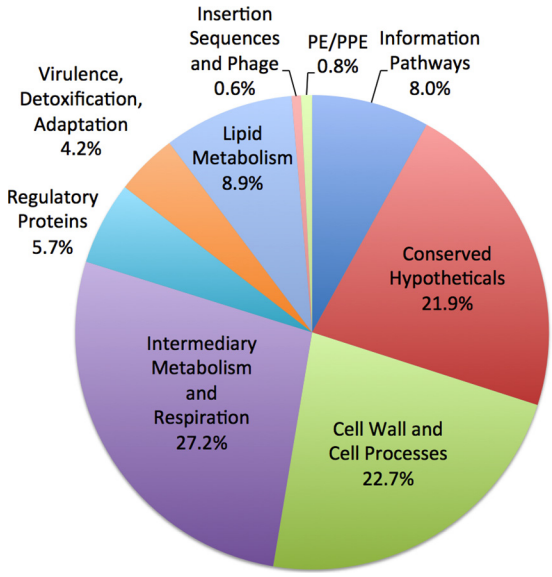

FIG. 1. **Functional categories of cell wall proteins identified by LC-MS/MS.** The 1729 cell wall-associated proteins identified by LC-MS/MS by a minimum of two peptides were assigned to functional categories according to Tuberculist (47).

intermediary metabolism/respiration, or are conserved hypothetical proteins (47). This distribution of cell wall-associated proteins among functional groups is similar to what is seen in other *M. tuberculosis* cell wall proteome studies (48, 49).

Of these 1729 proteins identified, 501 are predicted to be fully exported across or inserted into the cytoplasmic membrane because of the presence of a predicted Sec or Tat signal peptide (183 proteins) and/or a transmembrane domain (405 proteins). Additionally, 67 proteins were predicted to be lipoproteins, representing 70% of the lipoproteins predicted in the H37Rv genome (44), which is consistent with the role of lipidation in anchoring proteins to the bacterial cell envelope (50). The identification of proteins lacking a predicted signal peptide or transmembrane domain in the cell wall fraction was not surprising as past proteomic studies of mycobacterial membrane and cell wall fractions identify a similar percentage of proteins lacking export signals (31, 48, 49, 51, 52). Some of these proteins may be unconventional exported proteins lacking recognizable signals for export. However, because of the high sensitivity of mass spectrometry, cytoplasmic and cytoplasmic membrane contaminants can also be identified in the cell wall fraction.

Using spectral counting, we compared the composition and relative levels of proteins in the Δ*secA2* mutant to H37Rv cell wall fractions. Spectral counting is based on the observation that the total number of MS/MS spectra assigned to a protein correlates with the abundance of that protein (53). In order to avoid low abundance proteins that fall outside of the linear dynamic range of spectral counting, we limited our analysis to the 1318 proteins identified by a minimum of two peptides with an average of ≥four spectral counts (53) among the

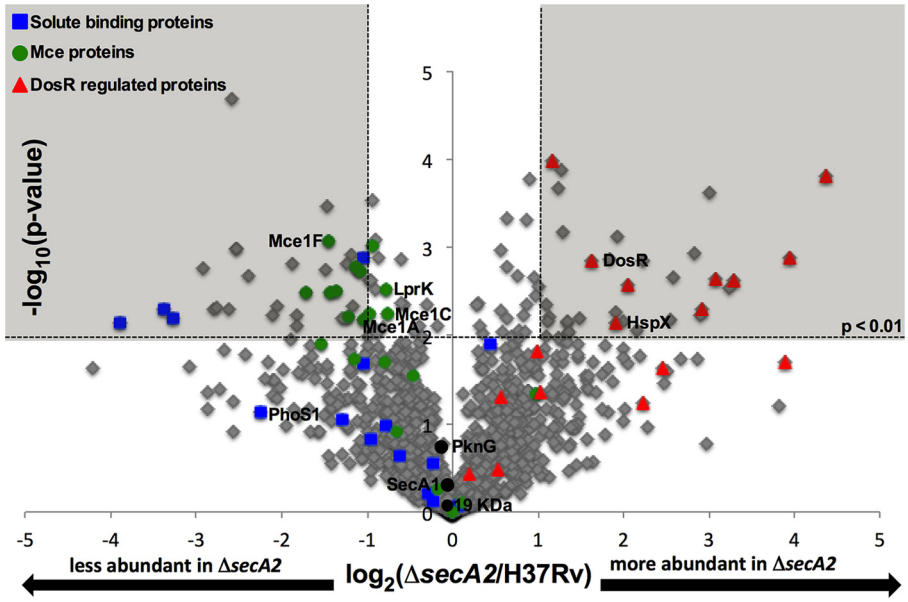

FIG. 2. **Relative quantitation of proteins in H37Rv and Δ*secA2* mutant cell wall-fractions.** Ratios for the 1300 proteins having average spectral counts of ≥4 in H37Rv and/or Δ*secA2* are shown plotted by $\log_2$ (Δ*secA2*/H37Rv) and $-\log_{10}$(*p* value). The shaded area of the graph indicates proteins showing twofold differences, $p < 0.01$. Solute binding proteins (blue squares), Mce transporter proteins (green circles), and DosR-regulated proteins (red triangles) are marked on the plot, and proteins later validated are identified. In addition, SecA1, is identified on the plot as a protein expected to be present in similar amounts between strains (54).

replicates of at least one of the strains (H37Rv or Δ*secA2* mutant) (supplemental Table S3). When the spectral count data for each replicate was compared, a good correlation was revealed between biological replicates (Pearson's correlation coefficient of r>0.92) (supplemental Fig. S1). Following normalization by total spectral counts for each protein, spectral count ratios ($\log_2$(Δ*secA2*/H37Rv)) were calculated for 1300 proteins that were detected in both strains (supplemental Table S3). For 18 proteins with average of ≥four spectral counts, spectral count ratios could not be calculated because these proteins were only identified in one of the two strains: Four proteins were exclusively identified in H37Rv (unidentified in the mutant) and 14 proteins were only identified in the Δ*secA2* mutant (supplemental Tables S4 and S5). Proteins exclusively identified in one of the strains are most likely present in the other strain, but at levels that fall below our limit of detection. For the 1300 proteins with spectral count ratios calculated, significant differences in protein levels between the two strains were determined by a Student's *t* test ($p < 0.01$) and by having a difference of twofold or greater between strains ($\log_2$ spectral count ratio of ±1.0). To visualize the distribution of spectral count ratios for the cell wall proteins, a volcano plot of the $\log_2$ ratio of Δ*secA2*/H37Rv *versus* $-\log_{10}$ *p* value was generated (Fig. 2). The majority of proteins were present at similar levels in the two strains. Of note, the SecA1 ATPase was detected at equivalent levels in the Δ*secA2* mutant and H37Rv (Fig. 2), which reinforces past conclusions that the absence of SecA2 does not alter the level of SecA1 (54). Among the proteins exhibiting significant differences (>twofold difference, $p < 0.01$), there were 33 proteins with significantly decreased levels in the cell wall fraction of the Δ*secA2* mutant *versus* H37Rv and 33 proteins with significantly increased levels in the Δ*secA2* mutant cell wall fraction relative to H37Rv (supplemental Tables S6 and S7). Proteins chosen for independent validation in this study are labeled on the volcano plot.

From the spectral counting analysis, we expected to detect protein abundance differences resulting from SecA2-dependent export defects as well as regulatory consequences of the absence of SecA2. Altogether, there were 37 proteins whose level was either reduced or unidentified in the Δ*secA2* cell wall when compared with H37Rv. Of these proteins, which represent candidates for being exported by the SecA2 pathway, 46% possess a predicted Sec or Tat signal peptide or putative transmembrane domain, with four of these proteins being predicted lipoproteins. Conversely, there were 47 proteins either increased or uniquely identified in the Δ*secA2* mutant compared with H37Rv. In this latter collection of proteins, there were a smaller percentage of predicted exported proteins (28%) and only one predicted lipoprotein. This latter group of proteins seems likely to include more examples of contaminating cytoplasmic proteins.

*Protein Families and Networks Exhibiting Differences in the Δ*secA2* Mutant versus H37Rv*—To identify functional categories and protein families that are SecA2-dependent we plotted the percentage of proteins in a given functional group, as defined by Tuberculist (47), that exhibited differential levels between the Δ*secA2* mutant and H37Rv (Fig. 3). However, none of these broad functional categories revealed a strong association with SecA2-dependent proteins (Fig. 3).

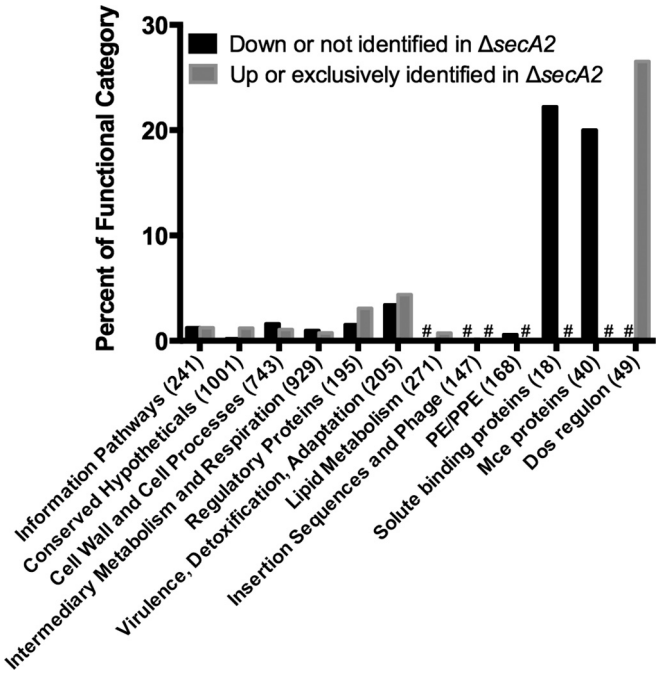

FIG. 3. **Percent of functional protein categories showing differences in the cell wall between H37Rv and the Δ*secA2* mutant.** Shown is the percent of proteins in a given functional category showing SecA2-dependence, defined as ≥twofold difference, $p < 0.01$ between H37Rv and Δ*secA2* or exclusively identified in one of the two strains (supplemental Tables S4–S7). With the exception of SBPs (44, 55), Mce transporters (representing Mce1–4 systems) (68), and DosR-regulated proteins (58), functional groups were predicted by Tuberculist (47). The total number of proteins in each functional category is denoted in parentheses. # indicates no proteins in that category.

Solute Binding Proteins (SBPs)—Because of the precedent of two *M. smegmatis* SBPs being SecA2-dependent exported proteins (15), we inspected the spectral counting data for the 15 SBPs we identified in the cell wall fraction (18 SBPs are predicted to exist in *M. tuberculosis*) (44, 55). This analysis revealed a trend in SBPs being reduced in the cell wall of the Δ*secA2* mutant when compared with H37Rv (Fig. 3; Table I). There were four SBPs significantly reduced (≥twofold decreased, $p < 0.01$) in the Δ*secA2* mutant cell wall compared with H37Rv. Furthermore, there were an additional nine SBPs reduced in the Δ*secA2* mutant cell wall, although the reduction relative to H37Rv did not always reach twofold or achieve statistical significance. All of these SBPs are predicted lipoproteins, which is consistent with their localization to the cell wall. Altogether, 13 of the 15 SBPs we identified were reduced to some degree in the Δ*secA2* mutant cell wall.

Mce Proteins—As an alternate approach to find functional categories or networks influenced by SecA2, we entered the SecA2-dependent proteins showing significant differences between strains (≥twofold difference, $p < 0.01$, or unidentified) (supplemental Tables S4–S7) into the Search Tool for the Retrieval of Interacting Genes (STRING) database of known and predicted protein associations (supplemental Figs. S2 and S3) (45). For clarity, Fig. 4 only shows portions of the STRING analysis. Among the proteins reduced/unidentified in the cell wall of the Δ*secA2* mutant *versus* H37Rv, there was a cluster of members of two of the four Mce transporter systems (Mce1 and Mce4) (Fig. 4*A*). When the percentage of all Mce transporter components showing differential abundance in the Δ*secA2* mutant *versus* H37Rv was plotted, the reduction in Mce protein family members in the Δ*secA2* cell wall was evident (Fig. 3).

Mce transporters are multiprotein complexes localized to the cell envelope (56, 57) that are proposed to function in lipid uptake by mycobacteria. Mce transporters are encoded by eight to 12 gene operons. Each system contains *yrbE* genes encoding putative membrane-spanning proteins, five *mce* genes encoding proteins with potential signal peptides or N-terminal transmembrane domains and one *lpr* gene encoding a lipoprotein (Fig. 5). Most Mce systems also have genes that encode Mce-associated proteins (*mas*) possessing transmembrane domains. Of the nine proteins encoded by the *mce4* locus, six proteins were significantly reduced in the Δ*secA2* mutant cell wall (≥twofold, $p < 0.01$) (Fig. 5, Table I). Mce4F and Mas4B were also reduced in the Δ*secA2* mutant, although the differences did not meet one or both of our cutoffs. Among the 12 components of the Mce1 system, six proteins were significantly reduced in the Δ*secA2* mutant cell wall ($p < 0.01$); however, only two of them (Mce1A and Mce1F) were reduced by ≥twofold. The Mce-associated ATPase MceG (MkI) was also significantly reduced in the Δ*secA2* mutant by 1.8-fold.

DosR-regulated Proteins—Among the proteins that were increased in the Δ*secA2* mutant relative to H37Rv, the STRING database identified a cluster of proteins that are members of the DosR regulon (58) (Figs. 3 and 4*B*). Of the 21 DosR-regulated proteins we identified, 13 were increased (≥twofold, $p < 0.01$) or exclusively identified in the Δ*secA2* cell wall. The mostly cytoplasmic proteins within the DosR regulon are under the transcriptional control of the DosR/S/T two component regulatory system. One of the proteins significantly increased in the Δ*secA2* mutant was the DosR response regulator, which is known to autoregulate itself at the transcriptional level (59). The remaining eight DosR-regulated proteins we identified in the cell wall followed the same trend of being increased in the Δ*secA2* mutant, although their differences failed to meet our significance and/or twofold cutoffs (Fig. 3, Table II).

Validation of Cell Wall Protein Differences—To validate the spectral counting identifications of the above families and networks of differentially abundant proteins, we performed immunoblot analysis on sets of newly prepared cell wall samples that included a complemented strain, which represents the Δ*secA2* mutant carrying a plasmid expressing wild type *secA2*. Using antibodies to PhoS1, we monitored the abundance of this representative SBP in the cell wall fractions of

TABLE I

Functional categories of proteins showing reduced abundance in the cell wall fraction of the M. tuberculosis ΔsecA2 mutant versus H37Rv. Shaded areas of the table indicate proteins that satisfied our criterion of having >twofold difference in abundance between the ΔsecA2 mutant and H37Rv and p < 0.01 or were exclusively identified in one of the strains

Sequence ID	Rv number	Gene name	Description	Total Peptides	Total Spectra	p value	q value	log2 (ΔsecA2/H37Rv)	Sec signal peptide	Tat signal peptide	Transmembrane domain	Lipoprotein
SOLUTE BINDING PROTEINS												
NP_216916.1	Rv2400c	subI	sulfate binding lipoprotein	3	15	0.007	0.060	-3.888				X
NP_218183.1	Rv3666c	dppA	peptide binding lipoprotein	8	32	0.005	0.055	-3.381	X		X	X
NP_214925.1	Rv0411c	glnH	glutamine binding lipoprotein	6	35	0.006	0.058	-3.270	X	X		X
NP_215796.1	Rv1280c	oppA	peptide binding lipoprotein	17	120	0.001	0.035	-1.051		X	X	X
YP_177705.1	Rv0265c	fecB2	iron (III) dicitratebinding lipoprotein	7	68	0.020	0.088	-1.037		X		X
NP_216557.1	Rv2041c		sugar binding lipoprotein	6	27	0.073	0.151	-2.256	X	X		X
YP_177770.1	Rv0934	phoS1	phosphate binding lipoprotein	13	765	0.090	0.172	-1.286	X			X
NP_217101.1	Rv2585c		peptide binding lipoprotein	12	70	0.150	0.234	-0.961	X			X
NP_217560.1	Rv3044	fecB	iron (III) dicitrate binding lipoprotein	10	121	0.104	0.190	-0.786	X			X
YP_177769.1	Rv0932c	pstS2	phosphate binding lipoprotein	11	147	0.232	0.299	-0.613	X			X
NP_218276.1	Rv3759c	proX	glycine/betaine/L-proline binding lipoprotein	6	37	0.628	0.516	-0.275	X			X
NP_215760.1	Rv1244	lpqZ	glycine/betaine binding lipoprotein	5	28	0.745	0.563	-0.231	X			X
NP_215751.1	Rv1235	lpqY	sugar binding lipoprotein	15	132	0.285	0.333	-0.224	X			X
NP_215682.1	Rv1166	lpqW	peptidebinding lipoprotein	12	109	0.861	0.603	0.062	X			X
YP_177768.1	Rv0928	pstS3	phosphate binding lipoprotein	7	49	0.013	0.078	0.443	X			X
MCE1												
NP_214681.1	Rv0167	yrbE1A	integral membrane protein YRBE1A	4	77	0.121	0.205	-0.662			X	
NP_214682.1	Rv0168	yrbE1B	integral membrane protein YRBE1B	3	23	0.019	0.086	-1.158			X	
YP_177701.1	Rv0169	mce1A	MCE-family protein MCE1A	18	431	0.007	0.058	-1.042			X	
NP_214684.1	Rv0170	mce1B	MCE-family protein MCE1B	19	667	0.020	0.088	-0.802			X	
NP_214685.1	Rv0171	mce1C	MCE-family protein MCE1C	31	774	0.006	0.058	-0.967	X		X	
NP_214686.1	Rv0172	mce1D	MCE-family protein MCE1D	19	638	0.001	0.035	-0.931			X	
NP_214687.1	Rv0173	lprK	MCE-family lipoprotein LprK	23	594	0.006	0.058	-0.770			X	X
NP_214688.1	Rv0174	mce1F	MCE-family protein MCE1F	19	837	0.002	0.036	-1.134			X	
NP_214689.1	Rv0175	mas1A	mce associated membrane protein	6	96	0.045	0.127	0.965			X	
NP_214690.1	Rv0176	mas1B	mce associated transmembrane protein	6	159	0.003	0.044	-0.772			X	
NP_214691.1	Rv0177	mas1C	MCE associated protein	10	135	0.543	0.479	-0.179			X	
NP_214692.1	Rv0178	mas1D	mce associated membrane protein	14	280	0.792	0.581	0.114			X	
MCE 4												
NP_218009.1	Rv3492c	mas4B	Mce associated protein	5	94	0.028	0.100	-0.469	X		X	
NP_218010.1	Rv3493c	mas4A	Mce associated alanine and valine rich protein	8	109	0.984	0.636	-0.007			X	
NP_218011.1	Rv3494c	mce4F	MCE-family protein MCE4F	9	85	0.013	0.078	-1.535			X	
NP_218012.1	Rv3495c	lprN	MCE-family lipoprotein LprN	14	153	0.003	0.046	-1.435				X
NP_218013.1	Rv3496c	mce4D	MCE-family protein MCE4D	12	102	0.003	0.046	-1.722			X	
NP_218014.1	Rv3497c	mce4C	MCE-family protein MCE4C	19	234	0.001	0.035	-1.458			X	
NP_218015.1	Rv3498c	mce4B	MCE-family protein MCE4B	14	123	0.006	0.058	-1.229	X		X	
YP_177977.1	Rv3499c	mce4A	MCE-family protein MCE4A	12	105	0.002	0.036	-1.071	X		X	
NP_218018.1	Rv3501c	yrbE4A	integral membrane protein YrbE4a	5	62	0.003	0.045	-1.370			X	

H37Rv, Δ*secA2*, and the complemented strain (Fig. 6*A*). As predicted by the spectral counting analysis, PhoS1 was partially reduced in the Δ*secA2* mutant cell wall. Importantly, the level of PhoS1 in the cell wall was restored in the complemented strain. PhoS1 levels in whole cell lysates were the same between strains (Fig. 6*B*) indicating that the reduced amount of PhoS1 in the Δ*secA2* cell wall is not caused by an effect on total PhoS1 levels. Rather, these results support PhoS1 being dependent on SecA2 for export to the cell wall. Using a series of antibodies to Mce1 components (Mce1A, Mce1C, Mce1F, and LprK) we similarly assessed the levels of Mce1 proteins in the cell wall. The levels of all four of these proteins were reduced in the cell wall of the Δ*secA2* mutant when compared with H37Rv and the complemented strain (Fig. 6*A*). In this case, lower levels of the Mce proteins were also observed in whole cell lysates of the Δ*secA2* mutant (Fig. 6*B*). Immunoblot analysis of cell wall fractions was also performed with anti19kDa lipoprotein antibodies. As predicted by the spectral counting data of cell wall fractions, the amount of the 19kDa lipoprotein was the same in the cell wall of all three strains.

We attempted immunoblot analysis with antibodies to HspX, as a representative DosR-regulated protein; however, the amount of HspX in the cell wall was below the level of detection. Therefore, in order to test the effect of SecA2 on HspX, we prepared samples from cultures that were left standing in 50 ml conical tubes for 2 or 24 h to induce DosR-dependent *hspX* expression (29). In these induced samples, HspX was detected in the cell wall and was present at higher levels in the Δ*secA2* mutant (Fig. 6*C*). Higher levels of HspX were also observed in the whole cell lysate as well as in the cytoplasm of the Δ*secA2* mutant indicating an overall increase in HspX levels in the Δ*secA2* mutant.

Transcriptional Effects do not Account for the Reduced Cell Wall Localization of Mce Proteins but can Account for DosR-regulated Effects—Genes in the *mce1* and *mce4* loci (Fig. 5) are organized in operons (61), which raises the possibility of a transcriptional effect accounting for the reduced levels of multiple Mce components that we observed in whole cell lysates and cell wall fractions of the Δ*secA2* mutant. To address the possibility of their being a transcriptional effect, we performed quantitative real time PCR (qRT-PCR) on RNA

prepared from H37Rv, Δ*secA2*, and complemented strains using primers for *mce1A, mce1F, mce4A*, and *mce4F*. Transcript levels were normalized to the housekeeping control *sigA* (46). For all four genes, there was no significant difference in transcript levels between H37Rv and the Δ*secA2* mutant (Fig. 7*A*). This result argues against a transcriptional effect on *mce* loci. Rather, it supports the alternate explanation for the immunoblot data, which is that there is a Mce export defect in the Δ*secA2* mutant and subsequent degradation of unexported Mce transporter components. In multiple experiments, the complemented strain showed a significantly lower level of *mce1A, mce1F, mce4F* transcript than either H37Rv or Δ*secA2*. The explanation for this effect is not clear, although it could reflect feedback regulation of *mce* expression in the presence of higher than normal SecA2 levels resulting from the complementation construct.

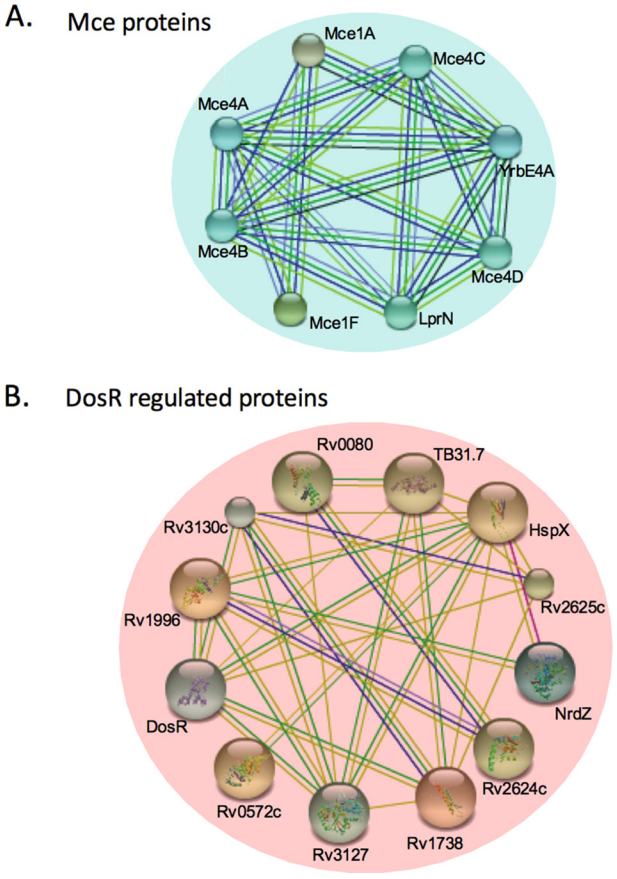

FIG. 4. **Protein associations among proteins identified as having differential abundance in the cell wall fractions of H37Rv *versus* the Δ*secA2* mutant.** *A*, Proteins that were less abundant (≤twofold, $p < 0.01$) or not identified in the Δ*secA2* mutant and *B* proteins that were more abundant (≥twofold, $p < 0.01$) or exclusively identified in the Δ*secA2* mutant were examined for protein associations. A portion of the protein associations predicted using the Search Tool for the Retrieval of Interacting Genes/Proteins (STRING) v9.1 using medium confidence are shown (45). Each line represents a different association between proteins.

The DosR-regulated proteins identified as more abundant in the Δ*secA2* mutant are all under transcriptional control of the DosR/S/T system. To test if SecA2 affects transcription of DosR-regulated genes we measured *hspX* transcript levels in H37Rv, Δ*secA2*, and complemented strains. RNA was prepared from uninduced samples and standing cultures that sat for 2 or 24 h to induce the DosR-regulon. In all conditions (± induction), the level of *hspX* transcript was higher in Δ*secA2 versus* H37Rv or the complemented strain (Fig. 7*B*). We also found that the level of *dosR* transcript was higher in the Δ*secA2* mutant, although the difference was only statistically significant after 2 h induction. Interestingly, in both the *hspX* and *dosR* transcript analyses the difference between H37Rv and Δ*secA2* samples was most pronounced at 2 h and waned at 24 h. Overall, these results indicate that the higher abundance of DosR-regulated proteins in the Δ*secA2* mutant can be attributed to increased transcription.

Proteomic Analysis of Differentially Abundant Proteins in the Cytoplasm of H37Rv versus the ΔsecA2 Mutant—Our detection of up-regulated cytoplasmic members of the DosR regulon in the Δ*secA2* mutant was fortuitous: A likely consequence of these proteins being highly expressed contaminants of cell wall fractions. To more directly test for cytoplasmic effects in the Δ*secA2* mutant, we performed LFQ analysis on cytoplasmic fractions prepared from triplicate H37Rv and Δ*secA2* mutant cultures. A total of 1810 proteins were identified by a minimum of two peptides among the cytoplasmic fractions of H37Rv and the Δ*secA2* mutant. As expected, proteins identified in the cytoplasmic fraction fall into diverse functional categories (Fig. 8*A*). As with the cell wall proteome, intermediary metabolism/respiration and conserved hypothetical proteins were among the largest functional groups of proteins identified in the cytoplasmic proteome. However, a much

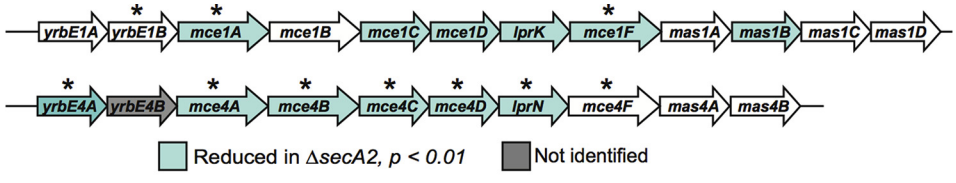

FIG. 5. **Multiple components of Mce1 and Mce4 transporters are reduced in the cell wall of the Δ*secA2* mutant.** The *M. tuberculosis* H37Rv genome contains four *mce* loci encoding putative lipid transporters. The genomic regions encoding Mce1 and Mce4 transporter components are shown with Open Reading Frames (ORF) colored for significant differences between strains of $p < 0.01$, as observed by spectral counting. An asterisk above the ORF indicates a difference of at least twofold.

TABLE II

DosR regulated proteins have altered abundance in the cell wall and cytoplasmic fractions of the M. tuberculosis ΔsecA2 mutant. Shaded areas of the table indicate proteins that satisfied our criterion of having >twofold difference in abundance between the ΔsecA2 mutant and H37Rv and $p < 0.01$ or were exclusively identified in one of the strains

				Cell Wall					Cytoplasm				
Sequence ID	Rv number	Gene name	Description	Total Peptides	Total Spectra	log2 (ΔsecA2/H37Rv)	p value	q value	Total Peptides	Total Spectra	log2 (ΔsecA2/H37Rv)	p value	q value
NP_214594.1	Rv0080		hypothetical protein Rv0080	4	34	1.9151	0.0073	0.0606	-	-	-	-	-
NP_215084.1	Rv0570	nrdZ	ribonucleoside-diphosphate reductase large subunit NrdZ	8	31	3.0784	0.0022	0.0385	-	-	-	-	-
NP_215086.1	Rv0572c		hypothetical protein Rv0572c	4	12	ΔsecA2 only	-	-	-	-	-	-	-
NP_216254.1	Rv1738		hypothetical protein Rv1738	3	30	3.2958	0.0023	0.0385	5	56	2.3085	0.0101	0.3424
NP_216512.1	Rv1996		hypothetical protein Rv1996	6	52	1.1671	0.0001	0.0175	10	66	2.0856	0.0089	0.3424
NP_216547.1	Rv2031c	hspX	heat shock protein hspX	8	173	2.0492	0.0026	0.0418	16	233	2.0544	0.0141	0.3646
NP_217139.1	Rv2623	TB31.7	hypothetical protein Rv2623	6	38	4.3776	0.0002	0.0175	20	294	2.5884	0.0125	0.3646
NP_217140.1	Rv2624c		hypothetical protein Rv2624c	4	18	ΔsecA2 only	-	-	5	15	ΔsecA2 only	-	-
NP_217141.1	Rv2625c		hypothetical protein Rv2625c	5	41	ΔsecA2 only	-	-	-	-	-	-	-
NP_217143.1	Rv2627c		hypothetical protein Rv2627c	8	55	3.9478	0.0013	0.0347	-	-	-	-	-
NP_217643.1	Rv3127		hypothetical protein Rv3127	6	22	ΔsecA2 only	-	-	14	103	6.5866	0.0002	0.0551
NP_217646.1	Rv3130c	tgs1	triacylglycerol synthase	13	86	2.9266	0.0049	0.0554	-	-	-	-	-
NP_217649.1	Rv3133c	dosR/devR	two component transcriptional regulatory protein DevR	3	22	1.6321	0.0014	0.0347	13	228	1.1133	0.0157	0.3896
NP_214593.1	Rv0079		hypothetical protein Rv0079	4	55	2.2214	0.0582	0.1400	-	-	-	-	-
NP_214595.1	Rv0081		transcriptional regulatory protein	-	-	-	-	-	5	39	0.4374	0.4681	0.8975
NP_215083.1	Rv0569		hypothetical protein Rv0569	-	-	-	-	-	4	65	2.5575	0.0031	0.2815
NP_216252.1	Rv1736c	narX	nitrate reductase NarX	6	99	1.0219	0.0436	0.1261	-	-	-	-	-
NP_216328.1	Rv1812c		dehydrogenase	6	47	0.1962	0.3793	0.3885	4	25	0.7515	0.2483	0.8020
NP_216519.1	Rv2003c		hypothetical protein Rv2003c	-	-	-	-	-	7	14	3.6192	0.0138	0.3646
NP_216520.1	Rv2004c		hypothetical protein Rv2004c	-	-	-	-	-	4	19	2.3486	0.0030	0.2815
NP_216521.1	Rv2005c		hypothetical protein Rv2005c	8	108	0.9888	0.0153	0.0843	15	111	2.0395	0.0309	0.4987
YP_177855.1	Rv2006	otsB1	trehalose-6-phosphate phosphatase	-	-	-	-	-	9	26	0.6305	0.3012	0.8306
NP_216523.1	Rv2007c	fdxA	ferredoxin FDXA	-	-	-	-	-	1	20	1.5136	0.0641	0.6161
NP_216544.1	Rv2028c		hypothetical protein Rv2028c	-	-	-	-	-	5	22	3.2650	0.0001	0.0509
NP_216546.1	Rv2030c		hypothetical protein Rv2030c	18	58	3.8953	0.0199	0.0878	16	70	3.6237	0.0049	0.2815
NP_216548.1	Rv2032	acg	hypothetical protein Rv2032	-	-	-	-	-	21	191	3.0202	0.0024	0.2815
NP_217142.1	Rv2626c		hypothetical protein Rv2626c	-	-	-	-	-	7	59	2.2287	0.0034	0.2815
NP_217145.1	Rv2629		hypothetical protein Rv2629	-	-	-	-	-	14	153	2.3547	0.00003	0.0299
NP_217647.1	Rv3131		hypothetical protein Rv3131	-	-	-	-	-	15	81	4.6169	0.0001	0.0299
NP_217648.1	Rv3132c	dosS/devS	two component sensor histidine kinase DEVS	16	150	0.5352	0.3297	0.3614	8	28	1.8222	0.0424	0.5412
NP_217650.1	Rv3134c		hypothetical protein Rv3134c	7	35	2.4513	0.0230	0.0917	7	40	4.1997	0.0022	0.2676
NP_218358.1	Rv3841	bfrB	bacterioferritin BfrB	6	108	0.5677	0.0501	0.1314	-	-	-	-	-

smaller percentage of proteins with predicted functions in cell wall processes were identified in the cytoplasm *versus* the cell wall (9.7% *versus* 22.7%), as expected.

Spectral count ratios were calculated for the 1266 proteins in the cytoplasmic fraction having average spectral counts ≥4 across the biological replicates of at least one of the strains. Once again, there was strong correlation between the spectral count data of replicates (Pearson's correlation coefficient of r>0.99 between replicate cytoplasmic fractions, as shown in supplemental Fig. S4). A volcano plot of the $\log_2$ ratio of Δ*secA2*/H37Rv shows the distribution of spectral count ratios (Fig. 8*B*). Among the proteins exhibiting significant differences (≥twofold, $p < 0.01$) between strains, there were 17 proteins with higher levels in the Δ*secA2* mutant and one protein with reduced levels of protein in the mutant. There were an additional three proteins with ≥4 average spectral counts that could not be quantitated because they were undetected in one of the two strains: two proteins were exclusively identified in Δ*secA2* mutant samples and SecA2 was the only protein exclusively identified in H37Rv. Of the proteins that were significantly increased or only identified in the Δ*secA2* mutant, 68% of them were DosR-regulated proteins (13 of 19 proteins) (Table II). As seen in the cell wall fractions, the other DosR-regulated proteins identified followed the same trend of being up-regulated in the Δ*secA2* mutant although the differences failed to meet our significance cut-offs. STRING analysis performed on proteins showing significant differences between strains (≥twofold difference, $p < 0.01$, or unidentified) identified no pathways, besides the DosR regulon, as being altered in the Δ*secA2* mutant.

PknG levels Are Increased in the Cytoplasm of the M. tuberculosis ΔsecA2 Mutant—Among the small number of non-DosR-regulated proteins detected at significantly higher levels in the cytoplasm of the Δ*secA2* mutant was the virulence factor PknG (6.1-fold increased, $p = 0.009$), which is reported to be SecA2-dependent in *M. marinum* (16). In some cases, when a protein is not being properly exported it will accumulate in the cytoplasm (15). Therefore, to follow up on this result, we performed immunoblot analysis with antiPknG antibodies on fractions prepared from H37Rv, Δ*secA2* mutant, and the complemented strain. Although PknG levels in the whole cell lysate were the same between the strains, the immunoblot confirmed a higher amount of PknG was present in the cytoplasmic fraction of the Δ*secA2* mutant (Fig. 9). Further, immunoblotting revealed less PknG in the cell wall fraction of the Δ*secA2* mutant when compared with H37Rv and the complemented strain. Therefore, although PknG did not meet our criteria of a significant difference in the LFQ

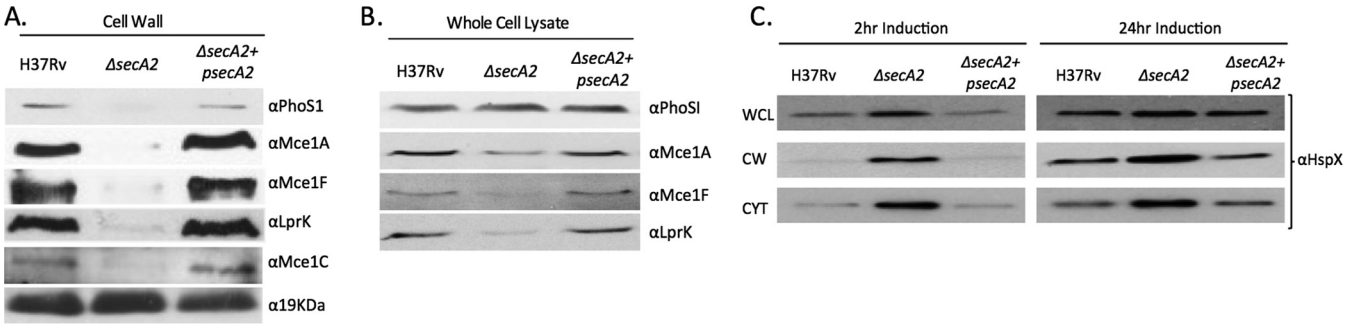

FIG. 6. **Immunoblot validation of protein abundance differences between H37Rv and the Δ*secA2* mutant.** *A*, Equalized cell wall fractions of H37Rv, Δ*secA2,* and complemented (Δ*secA2*+*psecA2*) strains were analyzed by immunoblot using antiPhoS1, antiMce1A, antiMce1C, antiMce1F, antiLprK, and anti19KDa antibodies to monitor differences in protein levels. The 19 kDa lipoprotein was used as a control for a protein present in equal amounts across the strains. *B*, Equalized whole cell lysates of H37Rv, Δ*secA2,* and complemented (Δ*secA2*+*psecA2*) strains were analyzed by immunoblot using antiPhoS1, antiMce1A, antiMce1F, and antiLprK antibodies. *C*, H37Rv, Δ*secA2,* and Δ*secA2*+*psecA2* samples in which the DosR regulon was induced for 2 or 24 h were analyzed. Whole cell lysate (WCL), cell wall (CW), and cytoplasmic (CYT) fractions were equalized for protein content and analyzed by immunoblot using antiHspX antibodies. For all data shown, a representative experiment is presented of a minimum of three that were performed.

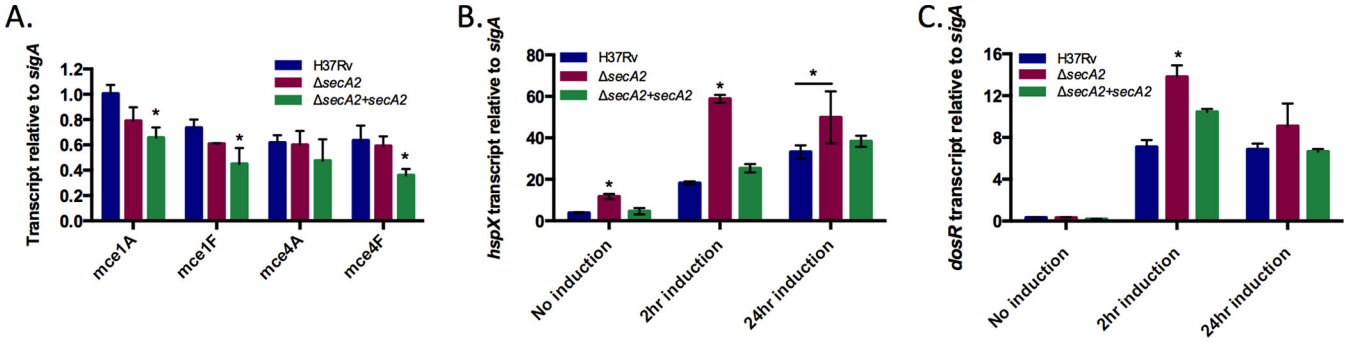

FIG. 7. **Transcript levels for *mce* genes are unchanged but transcript levels for DosR-regulated genes are higher in the Δ*secA2* mutant.** *A*, RNA was isolated from H37Rv, Δ*secA2,* and complemented (Δ*secA2*+*psecA2*) strains. *mce* transcript levels were measured by quantitative RT-PCR and normalized to the level of *sigA* transcript. Data shown is for the mean of three biological replicates. (*$p < 0.05$ by ANOVA) *B* and *C*, RNA was isolated from H37Rv, Δ*secA2,* and complemented (Δ*secA2*+*psecA2*) stains in which the DosR regulon was not intentionally induced or was induced for 2 or 24 h. *B*, *hspX* transcript levels and *C*, *dosR* transcript levels were measured by quantitative RT-PCR and normalized to *sigA* transcript. Data represents the means of three biological replicates. (*$p < 0.05$ by ANOVA).

analysis of the cell wall, our combined results from LFQ analysis of the cytoplasmic samples and immunoblot analysis are consistent with PknG being exported by the SecA2 pathway of *M. tuberculosis*, as reported to be the case for *M. marinum* (16).

DISCUSSION

Despite progress in understanding the mycobacterial SecA2 system, the identity of the proteins exported by the SecA2 pathway, most specifically of *M. tuberculosis*, has remained a critical unknown. Here, we took an unbiased proteomic approach using LFQ analysis with spectral counting to discover new proteins exported by the SecA2 pathway of *M. tuberculosis*. Using a cutoff of a ≥twofold difference and $p < 0.01$ we substantially increased the list of mycobacterial proteins observed to be affected by deletion of *secA2* (5, 15, 16). We mined this dataset to identify probable SecA2-dependent exported substrates and differences reflective of physiological effects of the SecA2 export pathway (Fig. 10). As with all proteomic studies of this sort, generating a comprehensive list of biologically significant differences is a challenge. Some differences and their significance will not be detected, as appears to have occurred for PknG in the cell wall analysis. Possible reasons for this occurring include quantitative measurement bias from missing data, incomplete sampling because of dynamic range issues, or matrix interference. At the same time, it is critical that differences detected in discovery experiments be validated with independently prepared samples, as performed for several proteins in this study.

Differences in Protein Families and Networks in the Δ*secA2 Mutant*—A striking observation from this study was the lower level of nearly all signal peptide-containing SBP lipoproteins identified (13 of 15) in the Δ*secA2* mutant *versus* H37Rv cell wall. Although the best-studied mycobacterial SecA2 substrates are *M. smegmatis* SBPs (15, 20, 21), this is the first demonstration of SecA2-dependent SBP export in *M. tuberculosis*. The reduction in SBP localization to the *M. tubercu-*

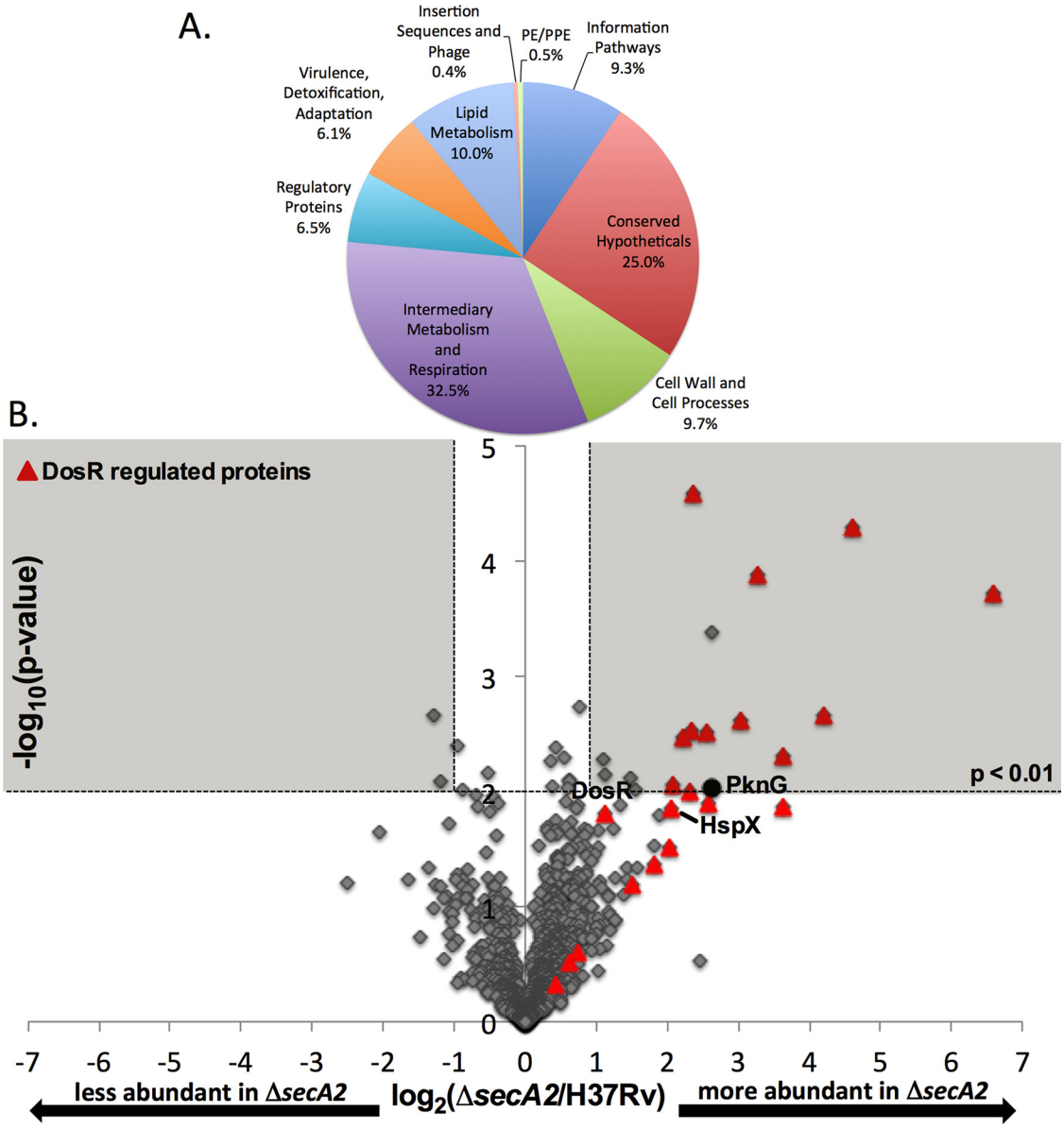

FIG. 8. **Relative quantitation of proteins in H37Rv and Δ*secA2* mutant cytoplasmic fractions.** *A*, The 1810 cytoplasmic proteins identified by LC-MS/MS by a minimum of two peptides were assigned to functional categories according to Tuberculist (47). *B*, Ratios for the 1266 proteins identified by an average ≥4 spectral counts in H37Rv and/or Δ*secA2* are shown plotted by $\log_2$ (Δ*secA2*/H37Rv) and $-\log_{10}$(*p* value). The shaded area of the graph indicates proteins showing twofold differences, $p < 0.01$. DosR-regulated proteins (red triangles) and PknG (black circle) are marked on the plot.

losis Δ*secA2* cell wall was not complete (*i.e.* residual export occurred in the absence of SecA2). However, partial export defects were also seen with other proteins identified in this study and in past studies of SecA2-dependent proteins of *M. tuberculosis, M.smegmatis,* and *M. marinum* (5, 15, 16). Our data argues for a general property of SBPs that imparts a requirement for SecA2 in their export. In support of this idea, three SBPs are among the proteins reduced in a proteomic study of the *M. marinum* cell envelope of a *secA2* mutant (16). An association of SBPs with SecA2-dependent export may also exist outside of mycobacteria. The *Listeria monocytogenes* SecA2-only system is reported to export three SBPs to the cell surface (14), although there are conflicting reports about the SecA2-dependent nature of some of these substrates (62, 63).

An interesting observation is that four of the 13 SBPs reduced in the *M. tuberculosis* Δ*secA2* mutant have predicted or proven Tat signal peptides (Table I) (39). The twin-arginine translocation (Tat) pathway operates independently and quite differently from the Sec pathway. The most notable feature of the Tat pathway is that it exports folded proteins across the cytoplasmic membrane (64). There are also examples of SBPs

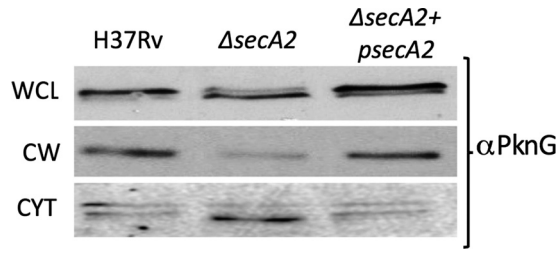

FIG. 9. **The level of PknG is increased in the cytoplasm and reduced in the cell wall of the Δ*secA2* mutant.** Equalized fractions of H37Rv, Δ*secA2,* and complemented (Δ*secA2*+*psecA2*) stains were analyzed by immunoblot using antiPknG antibodies. PknG levels in whole cell lysate (WCL), cell wall (CW), and cytoplasmic (CYT) fractions are shown. Shown is a representative of three experiments.

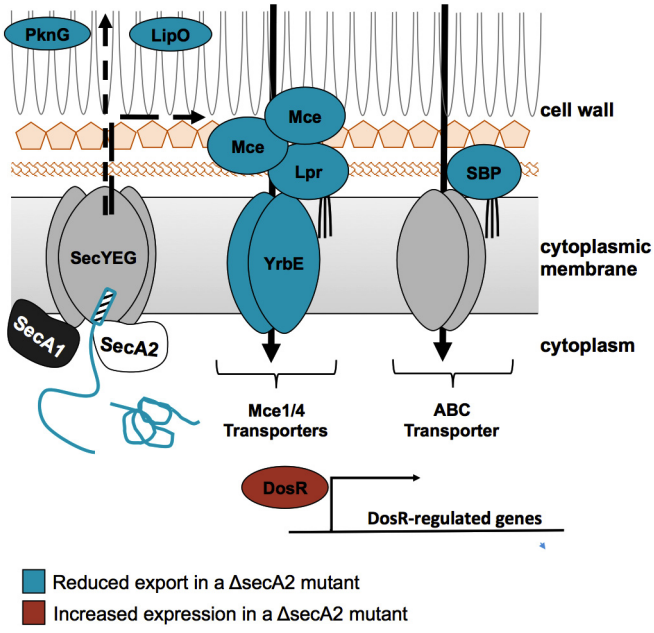

FIG. 10. **A model for SecA2-dependent effects in *M. tuberculosis*.** In the current model for SecA2-dependent protein export, the SecA2 ATPase promotes the export of select proteins across the cytoplasmic membrane through the SecYEG channel, possibly with the help of SecA1 (8, 19, 20). Proteins identified as being exported by the SecA2 pathway include examples with signal peptides (hatched rectangle) (*i.e.* SBPs) and examples lacking signal peptides (*i.e.* PknG). The SecA2-dependent proteins identified in this study are shown in the model with proteins identified as reduced in the Δ*secA2* mutant colored blue (*i.e.* PknG, SBPs, LipO, Mce, and Lpr) and proteins identified as increased in the Δ*secA2* mutant colored red (*i.e.* DosR-regulated proteins).

with Tat signal peptides in other bacteria, which suggests that cytoplasmic folding may be a common property of the SBP protein family (65, 66). A propensity for SecA2 exported proteins to fold in the cytoplasm is consistent with current models proposing a role for SecA2 in facilitating the export of such problematic proteins through the SecYEG channel that is built to accommodate proteins in an unfolded state (Fig. 10) (19, 21). These findings raise the possibility of at least some SBPs being compatible with Tat or SecA2 pathways, and for the Tat pathway being responsible for the residual export of SBPs that occurs in the absence of SecA2. It is important to note that only a subset of Tat substrates were SecA2-dependent in our study, ruling out a more general role for SecA2 in Tat export.

A new finding of this study was the effect of SecA2 on Mce1 and Mce4 transport systems. Because Mce2 or Mce3 proteins were not identified by an average of ≥four spectral counts, we do not know if other *M. tuberculosis* Mce systems depend on SecA2. However, reduced levels of LprM (Mce3E) as well as Mce4D were observed in the proteomic study of the *M. marinum secA2* mutant cell envelope suggesting export of other Mce systems may also depend on SecA2 (16). With qRT-PCR, we ruled out transcriptional effects being the cause of reduced Mce levels. The large number of exported Mce components reduced in the Δ*secA2* mutant could reflect a role for SecA2 in exporting numerous Mce transporter components. However it is also possible that SecA2 exports one or a small number of Mce components and that a defect in localizing a single Mce protein in the Δ*secA2* mutant destabilizes the entire complex. Along these lines, we identified reduced MceG levels in the Δ*secA2* mutant *versus* H37Rv. MceG is a predicted Mce-associated cytoplasmic ATPase and previous studies show MceG stability is influenced by the presence of Mce transporters (67). Mce systems are proposed to import lipids in a manner analogous to solute import by ABC transporters (68, 69). Furthermore, Mce and Lpr proteins have been considered functionally similar to the SBPs of ABC transporters (68, 69), making our identification of both SBPs and Mce proteins as SecA2-dependent an interesting similarity.

Our studies of cell wall and cytoplasmic fractions revealed increased induction of the DosR regulon in the Δ*secA2* mutant (58, 70). Although first identified as a coordinated response to hypoxia, a condition associated with *M. tuberculosis* latency, the DosR regulon is now appreciated as being induced by a number of stresses (29, 70–75). Standing cultures of *M. tuberculosis* are reportedly able to induce expression of DosR-regulated proteins, presumably because of hypoxic conditions for the settled bacteria (29). Our storage of cell pellets prior to irradiation and fractionation likely provided a DosR-inducing signal, revealing an unanticipated SecA2-dependent effect on this regulatory response. Using qRT-PCR, we showed increased transcription of DosR-regulated genes occurs in the Δ*secA2* mutant. Interestingly, with both *hspX* and *dosR* transcripts the fold difference observed in the Δ*secA2* mutant was greater at earlier times points and less dramatic at 24 h postinduction. Together, our results show increased transcription and possibly accelerated induction of the DosR regulon in the Δ*secA2* mutant. The Δ*secA2* mutant may be altered in a way that allows it to recognize or respond more quickly to DosR inducing stimuli. Alternatively, the absence of SecA2 could produce an underlying level of stress that primes the mutant for DosR induction, although our LFQ analysis of

cytoplasmic fractions did not reveal other stress pathways being up-regulated in the Δ*secA2* mutant. Our discovery of enhanced DosR responses could be useful for efforts to develop the *M. tuberculosis* Δ*secA2* mutant into a live attenuated vaccine (76, 77). Because of the desire for a tuberculosis vaccine to work with latent *M. tuberculosis* infections, a vaccine with improved ability to elicit immune responses to latency associated antigens, such as DosR-regulated proteins, would be advantageous (78).

SecA2-dependent Proteins with Functions in Virulence—SecA2 is required for growth and survival of *M. tuberculosis* in macrophages and mice (5–7). Although many differences detected by LFQ analysis remain to be validated, the results presented serve to expand the list of candidates to consider as SecA2-dependent effectors and help to develop new hypotheses for how SecA2 contributes to the pathogenesis of *M. tuberculosis*.

One way the SecA2 pathway functions in *M. tuberculosis* virulence is by enabling the bacterium to arrest phagosome maturation and avoid acidified phagolysosomes in macrophages (7). We identified two proteins that may help explain the role of *M. tuberculosis* SecA2 in arresting phagosome maturation. A predicted esterase LipO was significantly reduced in the Δ*secA2* mutant cell wall in comparison to H37Rv (6.9-fold reduced, $p = 0.005$). A *lipO (rv1426c)* mutant is defective in phagosome maturation arrest, indicating a potential role for LipO as an effector of this process (79). LipO has a predicted Sec signal peptide to account for its export to the cell wall. Although further studies are needed, our results raise the possibility of SecA2 localizing LipO to the cell wall and, thereby, enabling LipO to carry out a role in phagosome maturation arrest. An additional candidate for a being a SecA2 exported effector of phagosome maturation arrest is the protein kinase PknG, which is also implicated in phagosome maturation arrest (23). SecA2-dependent export of PknG likely contributes to phagosome maturation arrest, but there are probably additional SecA2-dependent effectors involved. This likelihood is supported by an experiment performed with the *M. marinum secA2* mutant that shows restoration of PknG export in a *secA2* mutant rescues some, but not all, phagosome maturation arrest in macrophages (16). Like the SecA2-dependent secreted SodA protein, PknG lacks an export signal. Thus, our results in support of PknG being exported by the SecA2 pathway of *M. tuberculosis* are also important in reinforcing earlier observations that SecA2-dependent substrates of mycobacteria include examples with and without signal peptides (5, 15, 16).

A role of SecA2 in exporting SBPs and Mce transporters may additionally contribute to *M. tuberculosis* virulence. Although most SBPs have yet to be investigated in terms of function, a wide range of solutes are predicted to be imported by these proteins. Collectively, the role of SecA2 in proper localization of SBPs could have a significant impact on nutrient acquisition or signaling during *M. tuberculosis* infection. Mce1 and Mce4 transporters are more firmly established as having roles in *M. tuberculosis* virulence. Although there is one conflicting report, multiple studies show Mce1 (like SecA2) is important for growth in macrophages and during the early phase of murine infection (5–7, 67, 80–83). The specific function of Mce1 during infection is not clear, but a potential role of Mce1 in importing free mycolic acids was recently proposed (57, 84). Mce4 is the best studied Mce transporter, with a shown role in cholesterol import (85, 86) and a role in virulence (85, 87). Thus, another way that the SecA2 pathway may contribute to *M. tuberculosis* infection could be through its role in SBP and Mce transporter localization.

CONCLUSION

Using a large-scale LFQ proteomic approach, we generated a list of candidates for cell wall proteins exported by the SecA2 pathway of *M. tuberculosis*. Our results are significant in highlighting SBPs as a family of SecA2-exported proteins and reinforcing prior observations that mycobacterial proteins exported in a SecA2-dependent fashion include examples with and without Sec signal peptides. At the same time, our results revealed unexpected contributions of SecA2 to Mce transport and DosR regulation. The proteins identified in this report represent a valuable resource for understanding the mechanism of SecA2-dependent export and contributions of this pathway to *M. tuberculosis* virulence and biology.

Acknowledgments—We thank Douglas Young, Murty Madiraju, and Yossef Av-Gay for providing antibodies and acknowledge members of the Braunstein laboratory and Dr. Henry S. Gibbons for critical reading the manuscript. We appreciate the assistance of Ellen Perkowski in assembling the bioinformatic predictions of export signals. The mass spectrometry proteomics data has been deposited to the ProteomeXchange Consortium with the dataset identifier PXD002144.

* Support for this study was provided to M.B. by NIAID AI054540.

Ⓢ This article contains supplemental Figs. S1 to S4 and Tables S1 to S15.

¶¶ Co-first authors.

** To whom correspondence should be addressed: Microbiology and Immunology, University of North Carolina at Chapel Hill, 6211 Marsico Hall Campus Box 7290 University of North Carolina, Chapel Hill, NC 27599. Tel.: 919-966-5051; Fax: 919-962-8103; E-mail: braunstein@med.unc.edu; Biochemistry and Biophysics, University of North Carolina at Chapel Hill, 3072 Genetic Medicine Building Campus Box 7260 University of North Carolinam, Chapel Hill, NC 27599. Tel.: 919-843-5310; Fax: 919-966-2852; E-mail: xchen@email.unc.edu.

REFERENCES

1. WorldHealthOrganization (2012) Global tuberculosis report 2012
2. Russell, D. G. (2008) *Mycobacterium tuberculosis:* life and death in the phagosome. In: Kaufmann, S. H., and Rubin, E. J., eds. *Handbook of Tuberculosis: Molecular Biology and Biochemistry*, pp. 307–322, Wiley-VCH
3. Hilbi, H., and Haas, A. (2012) Secretive bacterial pathogens and the secretory pathway. *Traffic* **13,** 1187–1197
4. Ligon, L. S., Hayden, J. D., and Braunstein, M. (2012) The ins and outs of Mycobacterium tuberculosis protein export. *Tuberculosis* **92,**

121–132
5. Braunstein, M., Espinosa, B., Chan, J., Belisle, J. T., and Jacobs, W. R. J. (2003) SecA2 functions in the secretion of superoxide dismutase A and in the virulence of *Mycobacterium tuberculosis*. *Mol. Microbiol.* **48,** 453–464
6. Kurtz, S., McKinnon, K. P., Runge, M. S., Ting, J. P., and Braunstein, M. (2006) The SecA2 secretion factor of *Mycobacterium tuberculosis* promotes growth in macrophages and inhibits the host immune response. *Infect. Immun.* **74,** 6855–6864
7. Sullivan, J. T., Young, E. F., McCann, J. R., and Braunstein, M. (2012) The *Mycobacterium tuberculosis* SecA2 system subverts phagosome maturation to promote growth in macrophages. *Infect. Immun.* **80,** 996–1006
8. Feltcher, M. E., and Braunstein, M. (2012) Emerging themes in SecA2-mediated protein export. *Nat. Rev. Microbiol.* **10,** 779–789
9. Bensing, B. A., Seepersaud, R., Yen, Y. T., and Sullam, P. M. (2014) Selective transport by SecA2: an expanding family of customized motor proteins. *Biochim. Biophys. Acta* **1843,** 1674–1686
10. Bensing, B. A., and Sullam, P. M. (2002) An accessory sec locus of *Streptococcus gordonii* is required for export of the surface protein GspB and for normal levels of binding to human platelets. *Mol. Microbiol.* **44,** 1081–1094
11. Siboo, I. R., Chaffin, D. O., Rubens, C. E., and Sullam, P. M. (2008) Characterization of the accessory Sec system of *Staphylococcus aureus*. *J. Bacteriol.* **190,** 6188–6196
12. Chen, Q., Wu, H., and Fives-Taylor, P. M. (2004) Investigating the role of secA2 in secretion and glycosylation of a fimbrial adhesin in *Streptococcus parasanguis* FW213. *Mol. Microbiol.* **53,** 843–856
13. Mistou, M. Y., Dramsi, S., Brega, S., Poyart, C., and Trieu-Cuot, P. (2009) Molecular dissection of the secA2 locus of group B *Streptococcus* reveals that glycosylation of the Srr1 LPXTG protein is required for full virulence. *J. Bacteriol.* **191,** 4195–4206
14. Lenz, L. L., Mohammadi, S., Geissler, A., and Portnoy, D. A. (2003) SecA2-dependent secretion of autolytic enzymes promotes *Listeria monocytogenes* pathogenesis. *Proc. Natl. Acad. Sci. U.S.A.* **100,** 12432–12437
15. Gibbons, H. S., Wolschendorf, F., Abshire, M., Niederweis, M., and Braunstein, M. (2007) Identification of two *Mycobacterium smegmatis* lipoproteins exported by a SecA2-dependent pathway. *J. Bacteriol.* **189,** 5090–5100
16. van der Woude, A. D., Stoop, E. J., Stiess, M., Wang, S., Ummels, R., van Stempvoort, G., Piersma, S. R., Cascioferro, A., Jimenez, C. R., Houben, E. N., Luirink, J., Pieters, J., van der Sar, A. M., and Bitter, W. (2014) Analysis of SecA2-dependent substrates in *Mycobacterium marinum* identifies protein kinase G (PknG) as a virulence effector. *Cell Microbiol.* **16,** 280–295
17. Fagan, R. P., and Fairweather, N. F. (2011) *Clostridium difficile* has two parallel and essential Sec secretion systems. *J. Biol. Chem.* **286,** 27483–27493
18. Rigel, N. W., and Braunstein, M. (2008) A new twist on an old pathway–accessory Sec systems. *Mol. Microbiol.* **69,** 291–302
19. Ligon, L. S., Rigel, N. W., Romanchuk, A., Jones, C. D., and Braunstein, M. (2013) Suppressor analysis reveals a role for SecY in the SecA2-dependent protein export pathway of mycobacteria. *J. Bacteriol.* **195,** 4456–4465
20. Rigel, N. W., Gibbons, H. S., McCann, J. R., McDonough, J. A., Kurtz, S., and Braunstein, M. (2009) The accessory SecA2 system of mycobacteria requires ATP binding and the canonical SecA1. *J. Biol. Chem.* **284,** 9927–9936
21. Feltcher, M. E., Gibbons, H. S., Ligon, L. S., and Braunstein, M. (2013) Protein export by the mycobacterial SecA2 system is determined by the preprotein mature domain. *J. Bacteriol.* **195,** 672–681
22. Watkins, B. Y., Joshi, S. A., Ball, D. A., Leggett, H., Park, S., Kim, J., Austin, C. D., Paler-Martinez, A., Xu, M., Downing, K. H., and Brown, E. J. (2012) *Mycobacterium marinum* SecA2 promotes stable granulomas and induces tumor necrosis factor alpha *in vivo*. *Infect. Immun.* **80,** 3512–3520
23. Walburger, A., Koul, A., Ferrari, G., Nguyen, L., Prescianotto-Baschong, C., Huygen, K., Klebl, B., Thompson, C., Bacher, G., and Pieters, J. (2004) Protein kinase G from pathogenic mycobacteria promotes survival within macrophages. *Science* **304,** 1800–1804
24. Cowley, S., Ko, M., Pick, N., Chow, R., Downing, K. J., Gordhan, B. G., Betts, J. C., Mizrahi, V., Smith, D. A., Stokes, R. W., and Av-Gay, Y. (2004) The *Mycobacterium tuberculosis* protein serine/threonine kinase PknG is linked to cellular glutamate/glutamine levels and is important for growth *in vivo*. *Mol. Microbiol.* **52,** 1691–1702
25. Rohde, K. H., Abramovitch, R. B., and Russell, D. G. (2007) *Mycobacterium tuberculosis* invasion of macrophages: linking bacterial gene expression to environmental cues. *Cell Host Microbe* **2,** 352–364
26. Schnappinger, D., Ehrt, S., Voskuil, M. I., Liu, Y., Mangan, J. A., Monahan, I. M., Dolganov, G., Efron, B., Butcher, P. D., Nathan, C., and Schoolnik, G. K. (2003) Transcriptional adaptation of *Mycobacterium tuberculosis* within macrophages: insights into the phagosomal environment. *J. Exp. Med.* **198,** 693–704
27. McKinney, J. D., Honer zu Bentrup, K., Munoz-Elias, E. J., Miczak, A., Chen, B., Chan, W. T., Swenson, D., Sacchettini, J. C., Jacobs, W. R., Jr., and Russell, D. G. (2000) Persistence of *Mycobacterium tuberculosis* in macrophages and mice requires the glyoxylate shunt enzyme isocitrate lyase. *Nature* 406, 735–738
28. Marrero, J., Rhee, K. Y., Schnappinger, D., Pethe, K., and Ehrt, S. (2010) Gluconeogenic carbon flow of tricarboxylic acid cycle intermediates is critical for *Mycobacterium tuberculosis* to establish and maintain infection. *Proc. Natl. Acad. Sci. U.S.A.* **107,** 9819–9824
29. Kendall, S. L., Movahedzadeh, F., Rison, S. C., Wernisch, L., Parish, T., Duncan, K., Betts, J. C., and Stoker, N. G. (2004) The *Mycobacterium tuberculosis* dosRS two-component system is induced by multiple stresses. *Tuberculosis* **84,** 247–255
30. Gu, S., Chen, J., Dobos, K. M., Bradbury, E. M., Belisle, J. T., and Chen, X. (2003) Comprehensive proteomic profiling of the membrane constituents of a *Mycobacterium tuberculosis* strain. *Mol. Cell. Proteomics* **2,** 1284–1296
31. Gunawardena, H. P., Feltcher, M. E., Wrobel, J. A., Gu, S., Braunstein, M., and Chen, X. (2013) Comparison of the membrane proteome of virulent *Mycobacterium tuberculosis* and the attenuated *Mycobacterium bovis* BCG vaccine strain by label-free quantitative proteomics. *J. Proteome Res.* **12,** 5463–5474
32. Elias, J. E., and Gygi, S. P. (2007) Target-decoy search strategy for increased confidence in large-scale protein identifications by mass spectrometry. *Nat. Methods* **4,** 207–214
33. Weatherly, D. B., Atwood, J. A., 3rd, Minning, T. A., Cavola, C., Tarleton, R. L., and Orlando, R. (2005) A heuristic method for assigning a false-discovery rate for protein identifications from Mascot database search results. *Mol. Cell. Proteomics* **4,** 762–772
34. Hsieh, E. J., Hoopmann, M. R., MacLean, B., and MacCoss, M. J. (2010) Comparison of database search strategies for high precursor mass accuracy MS/MS data. *J. Proteome Res.* **9,** 1138–1143
35. Keller, A., Nesvizhskii, A. I., Kolker, E., and Aebersold, R. (2002) Empirical statistical model to estimate the accuracy of peptide identifications made by MS/MS and database search. *Anal. Chem.* **74,** 5383–5392
36. Nesvizhskii, A. I., Keller, A., Kolker, E., and Aebersold, R. (2003) A statistical model for identifying proteins by tandem mass spectrometry. *Anal. Chem.* **75,** 4646–4658
37. Storey, J. D., and Tibshirani, R. (2003) Statistical significance for genome-wide studies. *Proc. Natl. Acad. Sci. U.S.A.* **100,** 9440–9445
38. Petersen, T. N., Brunak, S., von Heijne, G., and Nielsen, H. (2011) SignalP 4.0: discriminating signal peptides from transmembrane regions. *Nat. Methods* **8,** 785–786
39. McDonough, J. A., McCann, J. R., Tekippe, E. M., Silverman, J. S., Rigel, N. W., and Braunstein, M. (2008) Identification of functional Tat signal sequences in *Mycobacterium tuberculosis* proteins. *J. Bacteriol.* **190,** 6428–6438
40. Bendtsen, J. D., Nielsen, H., Widdick, D., Palmer, T., and Brunak, S. (2005) Prediction of twin-arginine signal peptides. *BMC Bioinformatics* **6,** 167
41. Rose, R. W., Bruser, T., Kissinger, J. C., and Pohlschroder, M. (2002) Adaptation of protein secretion to extremely high-salt conditions by extensive use of the twin-arginine translocation pathway. *Mol. Microbiol.* **45,** 943–950
42. Selengut, J. D., Haft, D. H., Davidsen, T., Ganapathy, A., Gwinn-Giglio, M., Nelson, W. C., Richter, A. R., and White, O. (2007) TIGRFAMs and Genome Properties: tools for the assignment of molecular function and biological process in prokaryotic genomes. *Nucleic Acids Res.* **35,** D260–264

43. Krogh, A., Larsson, B., von Heijne, G., and Sonnhammer, E. L. (2001) Predicting transmembrane protein topology with a hidden Markov model: application to complete genomes. *J. Mol. Biol.* **305,** 567–580
44. Sutcliffe, I. C., and Harrington, D. J. (2004) Lipoproteins of *Mycobacterium tuberculosis*: an abundant and functionally diverse class of cell envelope components. *FEMS Microbiol. Rev.* **28,** 645–659
45. Franceschini, A., Szklarczyk, D., Frankild, S., Kuhn, M., Simonovic, M., Roth, A., Lin, J., Minguez, P., Bork, P., von Mering, C., and Jensen, L. J. (2013) STRING v9.1: protein–protein interaction networks, with increased coverage and integration. *Nucleic Acids Res.* **41,** D808–815
46. Manganelli, R., Dubnau, E., Tyagi, S., Kramer, F. R., and Smith, I. (1999) Differential expression of 10 sigma factor genes in *Mycobacterium tuberculosis. Mol. Microbiol.* **31,** 715–724
47. Lew, J. M., Kapopoulou, A., Jones, L. M., and Cole, S. T. (2011) TubercuList–10 years after. *Tuberculosis* **91,** 1–7
48. Mawuenyega, K. G., Forst, C. V., Dobos, K. M., Belisle, J. T., Chen, J., Bradbury, E. M., Bradbury, A. R., and Chen, X. (2005) *Mycobacterium tuberculosis* functional network analysis by global subcellular protein profiling. *Mol. Biol. Cell* **16,** 396–404
49. Wolfe, L. M., Mahaffey, S. B., Kruh, N. A., and Dobos, K. M. (2010) Proteomic definition of the cell wall of *Mycobacterium tuberculosis*. *J. Proteome Res.* **9,** 5816–5826
50. Hutchings, M. I., Palmer, T., Harrington, D. J., and Sutcliffe, I. C. (2009) Lipoprotein biogenesis in Gram-positive bacteria: knowing when to hold 'em, knowing when to fold 'em. *Trends Microbiol.* **17,** 13–21
51. Malen, H., De Souza, G. A., Pathak, S., Softeland, T., and Wiker, H. G. (2011) Comparison of membrane proteins of *Mycobacterium tuberculosis* H37Rv and H37Ra strains. *BMC Microbiol.* **11,** 18
52. He, Z., and De Buck, J. (2010) Cell wall proteome analysis of *Mycobacterium smegmatis* strain MC2 155. *BMC Microbiol.* **10,** 121
53. Liu, H., Sadygov, R. G., and Yates, J. R., 3rd (2004) A model for random sampling and estimation of relative protein abundance in shotgun proteomics. *Anal. Chem.* 76, 4193–4201
54. Hou, J. M., D'Lima, N. G., Rigel, N. W., Gibbons, H. S., McCann, J. R., Braunstein, M., and Teschke, C. M. (2008) ATPase activity of *Mycobacterium tuberculosis* SecA1 and SecA2 proteins and its importance for SecA2 function in macrophages. *J. Bacteriol.* **190,** 4880–4887
55. Braibant, M., Gilot, P., and Content, J. (2000) The ATP binding cassette (ABC) transport systems of *Mycobacterium tuberculosis*. *FEMS Microbiol. Rev.* **24,** 449–467
56. Chitale, S., Ehrt, S., Kawamura, I., Fujimura, T., Shimono, N., Anand, N., Lu, S., Cohen-Gould, L., and Riley, L. W. (2001) Recombinant *Mycobacterium tuberculosis* protein associated with mammalian cell entry. *Cell Microbiol.* **3,** 247–254
57. Forrellad, M. A., McNeil, M., Santangelo Mde, L., Blanco, F. C., Garcia, E., Klepp, L. I., Huff, J., Niederweis, M., Jackson, M., and Bigi, F. (2014) Role of the Mce1 transporter in the lipid homeostasis of *Mycobacterium tuberculosis*. *Tuberculosis* **94,** 170–177
58. Park, H. D., Guinn, K. M., Harrell, M. I., Liao, R., Voskuil, M. I., Tompa, M., Schoolnik, G. K., and Sherman, D. R. (2003) Rv3133c/dosR is a transcription factor that mediates the hypoxic response of *Mycobacterium tuberculosis*. *Mol. Microbiol.* **48,** 833–843
59. Bagchi, G., Chauhan, S., Sharma, D., and Tyagi, J. S. (2005) Transcription and autoregulation of the Rv3134c-devR-devS operon of *Mycobacterium tuberculosis*. *Microbiology* **151,** 4045–4053
60. Boon, C., Li, R., Qi, R., and Dick, T. (2001) Proteins of *Mycobacterium bovis* BCG induced in the Wayne dormancy model. *J. Bacteriol.* **183,** 2672–2676
61. Kumar, A., Bose, M., and Brahmachari, V. (2003) Analysis of expression profile of mammalian cell entry (mce) operons of *Mycobacterium tuberculosis*. *Infect. Immun.* **71,** 6083–6087
62. Halbedel, S., Hahn, B., Daniel, R. A., and Flieger, A. (2012) DivIVA affects secretion of virulence-related autolysins in *Listeria monocytogenes*. *Mol. Microbiol.* **83,** 821–839
63. Renier, S., Chambon, C., Viala, D., Chagnot, C., Hebraud, M., and Desvaux, M. (2013) Exoproteomic analysis of the SecA2-dependent secretion in *Listeria monocytogenes* EGD-e. *J. Proteomics* **80C,** 183–195
64. Palmer, T., and Berks, B. C. (2012) The twin-arginine translocation (Tat) protein export pathway. *Nat. Rev. Microbiol.* **10,** 483–496
65. Shruthi, H., Babu, M. M., and Sankaran, K. (2010) TAT-pathway-dependent lipoproteins as a niche-based adaptation in prokaryotes. *J. Mol. Evol.* **70,** 359–370
66. Chater, K. F., Biro, S., Lee, K. J., Palmer, T., and Schrempf, H. (2010) The complex extracellular biology of *Streptomyces*. *FEMS Microbiol. Rev.* **34,** 171–198
67. Joshi, S. M., Pandey, A. K., Capite, N., Fortune, S. M., Rubin, E. J., and Sassetti, C. M. (2006) Characterization of mycobacterial virulence genes through genetic interaction mapping. *Proc. Natl. Acad. Sci. U.S.A.* **103,** 11760–11765
68. Casali, N., and Riley, L. W. (2007) A phylogenomic analysis of the Actinomycetales mce operons. *BMC Genomics* **8,** 60
69. Kumar, A., Chandolia, A., Chaudhry, U., Brahmachari, V., and Bose, M. (2005) Comparison of mammalian cell entry operons of mycobacteria: *in silico* analysis and expression profiling. *FEMS Immunol. Med. Microbiol.* **43,** 185–195
70. Sherman, D. R., Voskuil, M., Schnappinger, D., Liao, R., Harrell, M. I., and Schoolnik, G. K. (2001) Regulation of the *Mycobacterium tuberculosis* hypoxic response gene encoding alpha-crystallin. *Proc. Natl. Acad. Sci. U.S.A.* **98,** 7534–7539
71. Boon, C., and Dick, T. (2012) How *Mycobacterium tuberculosis* goes to sleep: the dormancy survival regulator DosR a decade later. *Future Microbiol.* **7,** 513–518
72. Shiloh, M. U., Manzanillo, P., and Cox, J. S. (2008) *Mycobacterium tuberculosis* senses host-derived carbon monoxide during macrophage infection. *Cell Host Microbe* **3,** 323–330
73. Kumar, A., Deshane, J. S., Crossman, D. K., Bolisetty, S., Yan, B. S., Kramnik, I., Agarwal, A., and Steyn, A. J. (2008) Heme oxygenase-1-derived carbon monoxide induces the *Mycobacterium tuberculosis* dormancy regulon. *J. Biol. Chem.* **283,** 18032–18039
74. Voskuil, M. I., Schnappinger, D., Visconti, K. C., Harrell, M. I., Dolganov, G. M., Sherman, D. R., and Schoolnik, G. K. (2003) Inhibition of respiration by nitric oxide induces a *Mycobacterium tuberculosis* dormancy program. *J. Exp. Med.* **198,** 705–713
75. Kumar, A., Toledo, J. C., Patel, R. P., Lancaster, J. R., Jr., and Steyn, A. J. (2007) *Mycobacterium tuberculosis* DosS is a redox sensor and DosT is a hypoxia sensor. *Proc. Natl. Acad. Sci. U.S.A.* 104, 11568–11573
76. Hinchey, J., Lee, S., Jeon, B. Y., Basaraba, R. J., Venkataswamy, M. M., Chen, B., Chan, J., Braunstein, M., Orme, I. M., Derrick, S. C., Morris, S. L., Jacobs, W. R., Jr., and Porcelli, S. A. (2007) Enhanced priming of adaptive immunity by a proapoptotic mutant of *Mycobacterium tuberculosis*. *J. Clin. Invest.* 117, 2279–2288
77. Hinchey, J., Jeon, B. Y., Alley, H., Chen, B., Goldberg, M., Derrick, S., Morris, S., Jacobs, W. R., Jr., Porcelli, S. A., and Lee, S. (2011) Lysine auxotrophy combined with deletion of the SecA2 gene results in a safe and highly immunogenic candidate live attenuated vaccine for tuberculosis. *PLoS One* **6,** e15857
78. Geluk, A., van Meijgaarden, K. E., Joosten, S. A., Commandeur, S., and Ottenhoff, T. H. (2014) Innovative strategies to identify *M. tuberculosis* antigens and epitopes using genome-wide analyses. *Front. Immunol.* **5,** 256
79. Pethe, K., Swenson, D. L., Alonso, S., Anderson, J., Wang, C., and Russell, D. G. (2004) Isolation of *Mycobacterium tuberculosis* mutants defective in the arrest of phagosome maturation. *Proc. Natl. Acad. Sci. U.S.A.* **101,** 13642–13647
80. McCann, J. R., McDonough, J. A., Sullivan, J. T., Feltcher, M. E., and Braunstein, M. (2011) Genome-wide identification of *Mycobacterium tuberculosis* exported proteins with roles in intracellular growth. *J. Bacteriol.* **193,** 854–861
81. Rengarajan, J., Bloom, B. R., and Rubin, E. J. (2005) Genome-wide requirements for *Mycobacterium tuberculosis* adaptation and survival in macrophages. *Proc. Natl. Acad. Sci. U.S.A.* **102,** 8327–8332
82. Gioffre, A., Infante, E., Aguilar, D., Santangelo, M. P., Klepp, L., Amadio, A., Meikle, V., Etchechoury, I., Romano, M. I., Cataldi, A., Hernandez, R. P., and Bigi, F. (2005) Mutation in mce operons attenuates *Mycobacterium tuberculosis* virulence. *Microbes Infect.* **7,** 325–334
83. Shimono, N., Morici, L., Casali, N., Cantrell, S., Sidders, B., Ehrt, S., and Riley, L. W. (2003) Hypervirulent mutant of *Mycobacterium tuberculosis* resulting from disruption of the mce1 operon. *Proc. Natl. Acad. Sci. U.S.A.* **100,** 15918–15923
84. Cantrell, S. A., Leavell, M. D., Marjanovic, O., Iavarone, A. T., Leary, J. A.,

and Riley, L. W. (2013) Free mycolic acid accumulation in the cell wall of the mce1 operon mutant strain of *Mycobacterium tuberculosis*. *J. Microbiol.* **51,** 619–626
85. Pandey, A. K., and Sassetti, C. M. (2008) Mycobacterial persistence requires the utilization of host cholesterol. *Proc. Natl. Acad. Sci. U.S.A.* **105,** 4376–4380
86. Klepp, L. I., Forrellad, M. A., Osella, A. V., Blanco, F. C., Stella, E. J., Bianco, M. V., Santangelo Mde, L., Sassetti, C., Jackson, M., Cataldi, A. A., Bigi, F., and Morbidoni, H. R. (2012) Impact of the deletion of the six mce operons in *Mycobacterium smegmatis*. *Microbes Infect.* **14,** 590–599
87. Senaratne, R. H., Sidders, B., Sequeira, P., Saunders, G., Dunphy, K., Marjanovic, O., Reader, J. R., Lima, P., Chan, S., Kendall, S., McFadden, J., and Riley, L. W. (2008) *Mycobacterium tuberculosis* strains disrupted in mce3 and mce4 operons are attenuated in mice. *J. Med. Microbiol.* **57,** 164–170